ACS Infectious Diseases

Article

Multistage Antiplasmodium Activity of Astemizole Analogues and Inhibition of Hemozoin Formation as a Contributor to Their Mode of Action

Malkeet Kumar, John Okombo, Dickson Mambwe, Dale Taylor, Nina Lawrence, Janette Reader, Mariëtte van der Watt, Diana Fontinha, Margarida Sanches-Vaz, Belinda C Bezuidenhout, Sonja Lauterbach, Dale Liebenberg, Lyn-Marie Birkholtz, Theresa L. Coetzer, Miguel Prudêncio, Timothy J Egan, Sergio Wittlin, and Kelly Chibale

ACS Infect. Dis., **Just Accepted Manuscript** • DOI: 10.1021/acsinfecdis.8b00272 • Publication Date (Web): 11 Dec 2018

ACS Publications

is published by the American Chemical Society. 1155 Sixteenth Street N.W., Washington, DC 20036

Multistage Antiplasmodium Activity of Astemizole Analogues and Inhibition of Hemozoin Formation as a Contributor to Their Mode of Action

Malkeet Kumar[1], John Okombo[1], Dickson Mambwe[1], Dale Taylor[2], Nina Lawrence[2], Janette Reader[3], Mariëtte van der Watt[3], Diana Fontinha[4], Margarida Sanches-Vaz[4], Belinda C Bezuidenhout[5], Sonja B Lauterbach[5], Dale Liebenberg[5], Lyn-Marie Birkholtz[3], Theresa L Coetzer[5], Miguel Prudêncio[4], Timothy J. Egan[1,6], Sergio Wittlin[7,8], Kelly Chibale[1,6,9]*

[1]Department of Chemistry, University of Cape Town, Rondebosch 7701, South Africa.

[2]Drug Discovery and Development Centre (H3D), Division of Clinical Pharmacology, Department of Medicine, University of Cape Town, Observatory 7925, South Africa.

[3]Department of Biochemistry, Genetics and Microbiology, Institute for Sustainable Malaria Control, University of Pretoria, Private Bag X20, Hatfield 0028, South Africa.

[4]Instituto de Medicina Molecular, Faculdade de Medicina, Universidade de Lisboa, Av. Prof. Egas Moniz, 1649-028 Lisboa, Portugal.

[5]Department of Molecular Medicine and Haematology, School of Pathology, Faculty of Health Sciences, University of the Witwatersrand and National Health Laboratory Service, Johannesburg 2193, South Africa

[6]Institute of Infectious Disease and Molecular Medicine, University of Cape Town, Rondebosch 7701, South Africa.

[7]Swiss Tropical and Public Health Institute, Socinstrasse 57, 4002 Basel, Switzerland

[8]University of Basel, 4003 Basel, Switzerland.

[9]South African Medical Research Council Drug Discovery and Development Research Unit, Department of Chemistry University of Cape Town, Rondebosch 7701, South Africa.

*Corresponding Author: Kelly Chibale

Email: Kelly.Chibale@uct.ac.za: Phone: +27-21-6502553. Fax: +27-21-6505195.

A drug repositioning approach was leveraged to derivatize astemizole (AST), an antihistamine drug whose antimalarial activity was previously identified in a high-throughput screen. The multistage activity potential against *Plasmodium* parasite's life cycle of the subsequent analogues was examined by evaluating against the parasite asexual blood, liver and gametocyte stages. In addition, the previously reported contribution of heme detoxification to the compound's mode of action was interrogated. Ten of the seventeen derivatives showed IC_{50}s < 0.1 μM against the chloroquine (CQ)-sensitive *Plasmodium falciparum* NF54 (*Pf*NF54) strain while maintaining submicromolar potency against the multidrug resistant strain, *Pf*K1, with most showing low likelihood of cross-resistance with CQ. Selected analogues (*Pf*NF54- IC_{50} < 0.1 μM) were tested for cytotoxicity on CHO cells and found to be highly selective (selectivity index > 100). The first ever gametocytes screening of AST and its analogues revealed their moderate activity (IC_{50}: 1 – 5 μM) against late stage *P. falciparum* gametocytes, while the evaluation of activity against *P. berghei* liver stages identified one compound (**3**) with three-fold greater activity than the parent AST compound. Mechanistic studies showed a strong correlation between *in vitro* inhibition of β-haematin formation by the AST derivatives and their antiplasmodium IC_{50}s. Analyses of intracellular inhibition of hemozoin formation within the parasite further yielded signatures attributable to a possible perturbation of the heme detoxification machinery.

Key Words: Astemizole, Repositioning, *Plasmodium falciparum*, β-haematin, Gametocytes

The latest statistics from the World Health Organization estimate that there were 216 million cases and 445,000 deaths due to malaria in 2016.[1] While these numbers mirror a trend of declining malaria burden over the past 15 years due to control strategies, which comprise indoor residual spraying, insecticide-treated nets, intermittent preventive treatments and adoption of artemisinin combinations as first-line therapy, the disease still remains a major public health concern. In fact, the recent evolution and dissemination of artemisinin-tolerant *Plasmodium falciparum* strains and suboptimal response to insecticides used for management of the *Anopheles* vector threaten the ultimate success of these control efforts.[2,3] To minimize the likelihood of rapid development of drug resistance, there is a clear need for innovation in order to identify safe and effective antimalarial compounds that can preferably inhibit multiple stages of the parasite's life cycle, which includes the asexual erythrocytic blood stage, the transmissible sexual gametocytic stage and a hepatocytic liver stage . One attractive approach to novel antimalarial drug design that can significantly reduce the pitfalls inherent to drug development is the repositioning of already-approved pharmacotherapies – a strategy whose application in malaria and neglected tropical diseases has been reviewed elsewhere.[4]

In the search for new drugs to treat malaria, researchers at Johns Hopkins University (JHU), in 2006, screened a chemical library comprising 2 687 Food and Drug Administration (FDA)-approved drugs for potential inhibitors of *P. falciparum* proliferation. This led to the discovery of antiplasmodium properties of astemizole (AST) (**Figure 1**), a second-generation antihistamine, which was withdrawn from market due to cardiotoxicity caused by its hERG channel blocking

activity and association with arrhythmias.[5] In that study, AST exhibited submicromolar half-maximal inhibitory concentrations (IC_{50}s) against three *P. falciparum* strains with different levels of chloroquine (CQ) sensitivity.[5] In humans, AST is rapidly absorbed from the gastrointestinal tract and undergoes extensive first-pass metabolism to the pharmacologically active desmethylastemizole (DM-AST) and other minor metabolites, including nor-astemizole (Nor-AST) (**Figure 1**).[6] Incidentally, these metabolites also exhibited antiplasmodium activity in the JHU screen, with DM-AST showing two- to twelve-fold higher potency than AST, depending on the parasite strain (**Figure 1**).[5] Further evaluation revealed their antimalarial potential, with 80% and 81% suppression of parasitaemia in *P. vinckei*-infected mice treated for four days with AST (30 mg/m^2/day) and DM-AST (15 mg/m^2/day), respectively.[5]

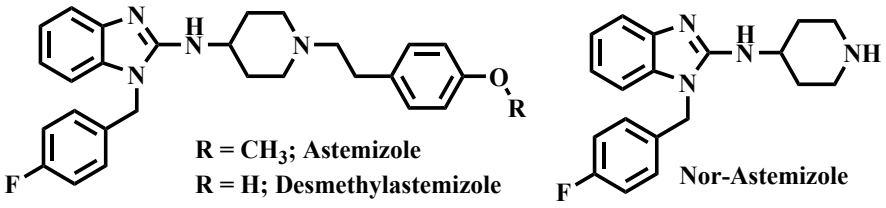

***Pf*3D7/*Pf*Dd2/*Pf*ItG**
AST-IC_{50} (µM) = 0.23/0.46/0.73
DM-AST-IC_{50} (µM) = 0.12/0.11/0.06
Nor-AST-IC_{50} (µM) = 4.48/3.60/2.23
CQ-IC_{50} (µM) = 0.03/0.08/0.11

Figure 1: Chemical structures and antiplasmodium activity of AST and its metabolites as reported by Chong *et al* (2006) against *Pf*3D7, *Pf*Dd2 and *Pf*ItG strains.[5]

Encouragingly, the antimalarial potential of AST has been recently investigated by other researchers. Employing a conjugated approach that hybridized CQ and AST structural motifs, Musonda *et al.* reported on CQ-AST hybrid compounds with *in vitro* activity against CQ-resistant (CQR) strains and *in vivo* activity in a murine malaria model.[7] Similarly, Roman and colleagues

reported on potent AST derivatives bearing several modifications to the AST structure against the CQR *P. falciparum* strain, ItG.[8] More recently, Tian and co-workers identified AST derivatives that showed good activity against the CQS strain, *Pf*3D7, and exhibited reduced hERG channel inhibition potency.[9] Various known chemical modification strategies can be employed to mitigate hERG channel inhibition activity in new AST analogues. These include (a) reduction of lipophilicity *via* removal of aromatic groups as already demonstrated in case of AST[9], reduction in the clogP via incorporation of polar moieties and heteroaromatic replacement of aromatic groups; (b) attenuation of pKa *via* modulation of the basicity of a nitrogen atom; (c) incorporation of three dimensional character and reduction in π-π stacking interactions. While these studies focused solely on the inhibition of asexual blood stage parasite proliferation, Derbyshire and co-workers further reported on the effectiveness of AST in a high-throughput phenotypic screen developed to systematically identify molecules with liver-stage efficacy.[10]

The basic premise of the drug repositioning approach involves further re-engineering of the original molecule for optimization into a new chemical entity with improved potency, physicochemical profile and/or safety. Although, the findings from the seminal JHU screen have been pursued by others to highlight the antimalarial potential of AST, to our knowledge no medicinal chemistry effort to date has focused on probing the multistage antiplasmodium activity of AST analogues across liver, asexual blood and gametocytic life-cycle stages. As an extension to our group's efforts aimed at identifying multistage active antiplasmodium compounds, this article explores structural modifications around the core AST pharmacophore (**Figure 2**) in anticipation of developing analogues with favourable solubility and cytotoxicity indices, as well as activity against different stages of the parasite's life cycle. This involved i) amending the central part of AST through replacement of the 4-aminopiperidine moiety with a piperazine; ii) modifying

the left hand side (LHS) of AST by a) complete removal of the benzyl group and replacing it with a methyl or b) replacing the fluoro moiety with, methyl ketone, cyano, acid, amide, sulfonyl and pyridyl nitrogen or c) regio-isomers of the fluoro- and cyano-substituted benzyl group; and iii) regio-isomerization of the methoxy substituent or replacement of the 4-methoxyphenyl with 4-hydroxyphenyl on the right hand side (RHS) of AST. Some of the analogues with modifications on LHS of AST such as complete removal of the benzyl group and its replacement with a methyl group as well as replacement of fluoro substituent on benzyl moiety with amide, sulfonyl, acid and pyridyl groups were also aimed at reducing lipophilicity (cLogP < 4.5 vs AST cLogP of 5.84; Supplementary Information Table S1).

During *Plasmodium* blood stage infection, host haemoglobin (Hb) is degraded into globin as a nutrient source, and heme is released as a by-product of this obligate catabolism. However, in its free state, heme is toxic as it can induce free radical formation as well as membrane damage.[11,12] To bypass this toxicity, *P. falciparum* converts heme into insoluble hemozoin (Hz) crystals - a detoxification process known to be inhibited by quinolines such as CQ and one that is tractable using *in vitro* models which mimic the digestive vacuole (DV) milieu. In line with previous findings showing that AST and DM-AST concentrate within the parasite's DV, inhibit heme crystallization and co-purify with Hz in drug-sensitive and resistant parasites,[5] we also queried the contribution of inhibition of heme detoxification as at least one of the possible modes of action (MoA) of AST.

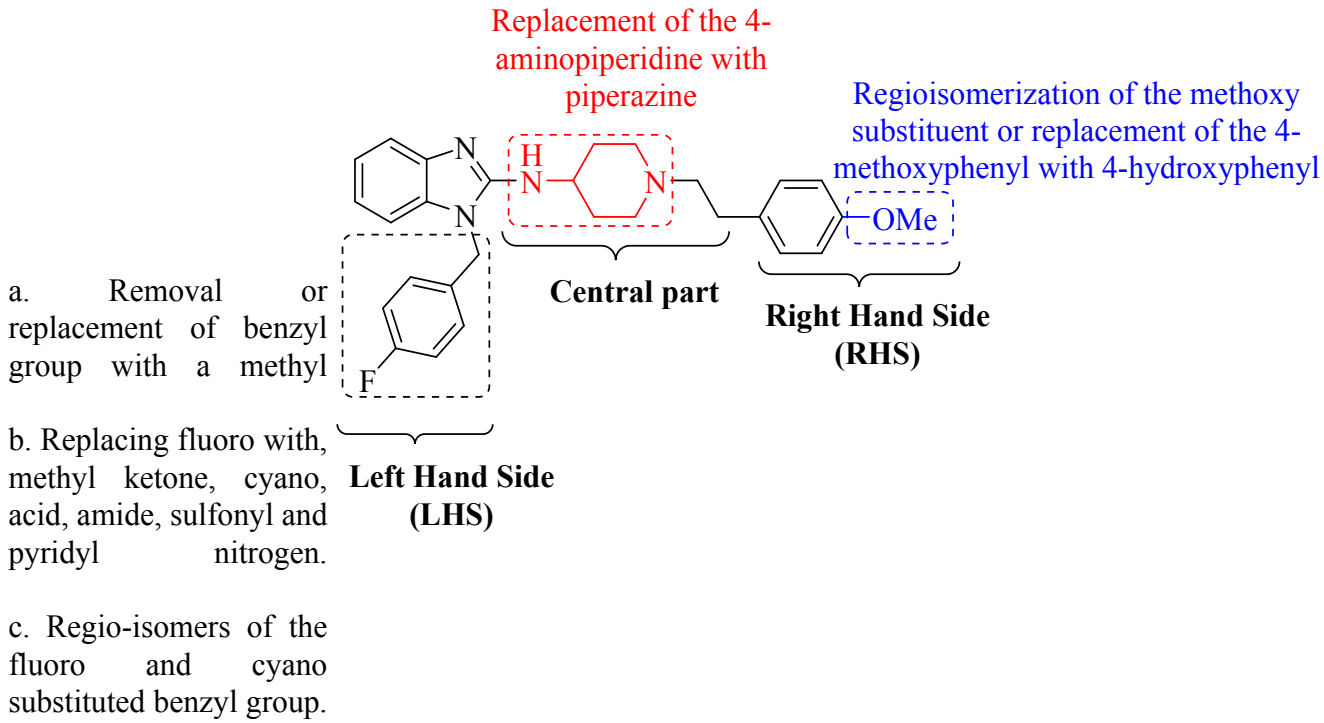

Figure 2: Structural modifications around AST to design various derivatives

CHEMISTRY: The synthesis of AST analogues is summarized in **Scheme 1**. AST analogue **3** with the piperazinyl moiety replacing AST's amino piperidinyl moiety was synthesized in two steps, a reaction of commercially available **1b** with piperazine followed by 1-(2-bromoethyl)-4-methoxybenzene. The synthesis of compounds **7-16** commenced with the benzylation of commercially available 2-chlorobenzimidazole (**1a**) using K_2CO_3 in acetone to afford intermediates **4a-j**, which were subsequently reacted with 1-(4-methoxyphenethyl)piperidin-4-amine in a neat reaction at 170 °C to obtain AST analogues **7-16**. AST was obtained by direct reaction of **1b** with 1-(4-methoxyphenethyl)piperidin-4-amine while the demethylation of AST using HBr afforded DM-AST.

The synthesis of compounds **17-20** began with the reaction of **1a, b** with protected 4-aminopiperidines to afford intermediate **5a, b** (**Scheme 1**). The benzylation of **5a** with 4-(bromomethyl)benzonitrile followed by deprotection using 4M HCl in dioxane afforded **6a**, while Nor-AST was obtained by direct deprotection of **5b**. The reaction of **6a** and Nor-AST with the respective phenyl ethyl bromide using K_2CO_3 in acetonitrile at reflux resulted in compounds **17-20** (**Scheme 1**). The AST analogue **5c** was obtained by direct reaction of **1a** with 1-(4-methoxyphenethyl)piperidin-4-amine. On the other hand, **1a** was first *N*-methylated and then reacted with 1-(4-methoxyphenethyl)piperidin-4-amine to afford analogue **5d**.

Scheme 1: Synthesis of AST analogues

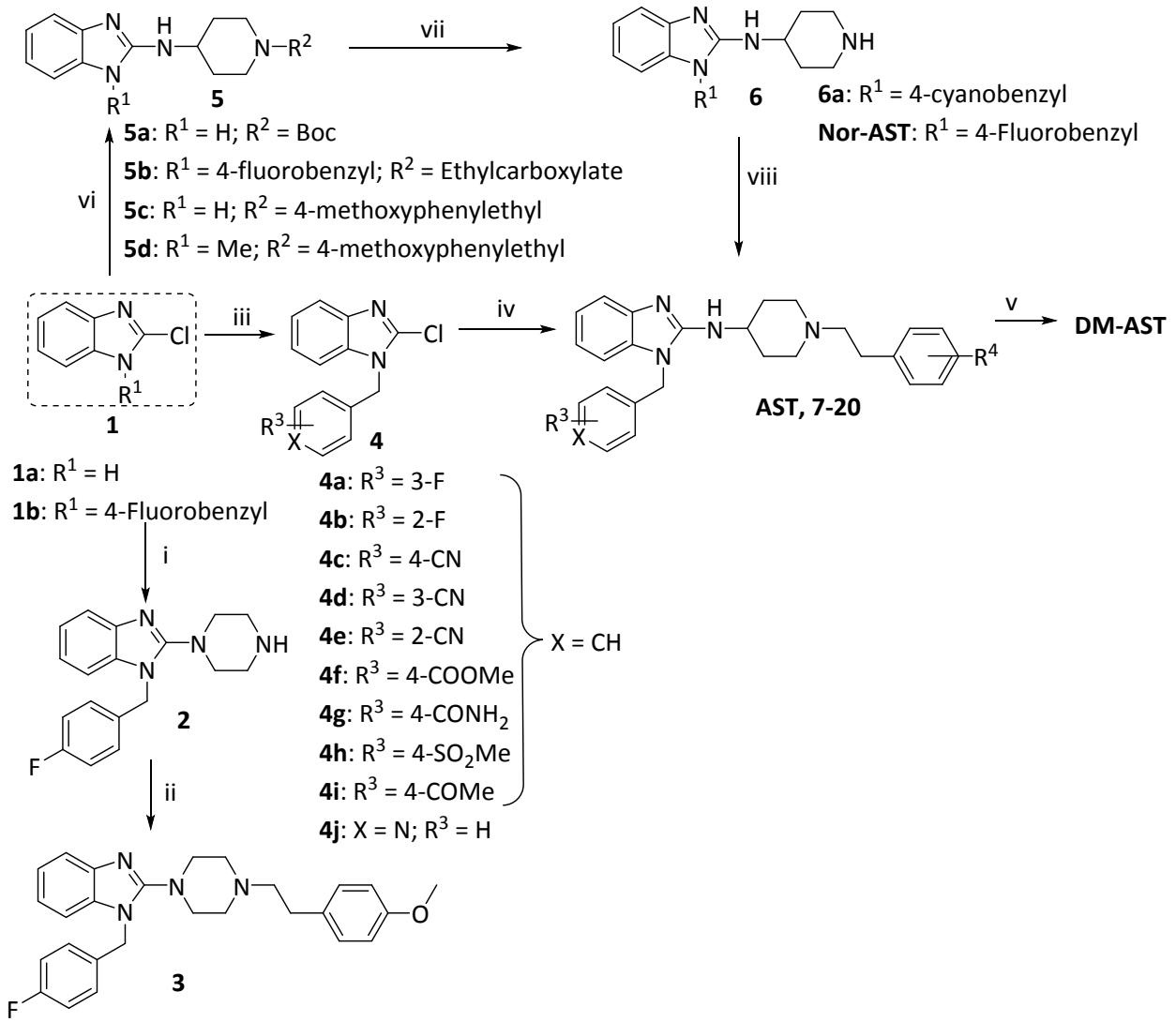

Reagents and conditions: (i) **1b**, piperazine, Et_3N, *t*-BuOH, 120 °C, 48 h, 87%; (ii) 1-(2-bromoethyl)-4-methoxybenzene, toluene, reflux, 48 h, 50%; (iii) **1a**, appropriate benzyl halide, K_2CO_3, acetone, 23 °C, 4-6 h, 70-85% (**4a-j**); (iv) 1-(4-methoxyphenethyl)piperidin-4-amine, 170 °C, 6-12 h, 15-74% (AST, **7-16**); (v) AST, HBr, reflux (120 °C), 6 h, 48%; (vi) **1a**, 4-amino-N-boc-piperidine, TEA, 150 °C, 2 h, 60% (**5a**); **1b**, ethyl 4-aminopiperidine-1-carboxylate, 170 °C, 4 h, 98% (**5b**); 1-(4-methoxyphenethyl)piperidin-4-amine, 170 °C, 4 h, 48% (**5c**); (a) **1a**, methyl iodide, K_2CO_3, acetone, 23 °C, 30 min, 68%; (b) 1-(4-methoxyphenethyl)piperidin-4-amine, 170

°C, 8 h, 30% (**5d**); (vii) (a) **5a**, 4-(2-bromomethyl)benzonitrile, K_2CO_3, DMF, 70 °C, 3 h, 88%; (b) 4N HCl in dioxane, 18 °C, 2 h, 80% (**6a**); **5b**, HBr, reflux (120 °C), 6 h, 85% (Nor-AST); (viii) **6a**, 4-(2-bromoethyl)phenol, K_2CO_3, ACN, 79 °C, reflux (85 °C), 5 h, 36%; (**17**); Nor-AST, 1-(2-bromoethyl)-3-methoxybenzene, ACN, reflux (85 °C), 16 h, 78% (**18**); Nor-AST, 1-(2-bromoethyl)-2-methoxybenzene, ACN, reflux (85 °C), 24 h, 71% (**19**); Nor-AST, (2-bromoethyl)benzene, ACN, reflux (85 °C), 12 h, 79% (**20**).

RESULTS & DISCUSSION:

Blood Stage Antiplasmodium Activity, **Cytotoxicity and Solubility**:

The antiplasmodium activity of AST, DM-AST, Nor-AST and all newly synthesized analogues was evaluated against the CQ sensitive *Pf*NF54 strain. Compounds with sub-micromolar potency against *Pf*NF54 were further tested against the multidrug resistant *Pf*K1 strain. Additionally, solubility of all the compounds was determined while analogues with $IC_{50} \leq 0.1$ μM against *Pf*NF54 were also tested for cellular toxicity against CHO cells (**Table 1**).

Replacing the amino piperidine in the central core of the AST structure with piperazine (**3**) did not increase antiplasmodium activity (*Pf*NF54-IC_{50} = 1.9 μM), as the resulting compound exhibited comparably less activity than AST (*Pf*NF54-IC_{50} = 0.086 μM). The structural changes on the LHS of the molecule showed that the benzyl group is not important for the activity, as the debenzylated analogue **5c** (*Pf*NF54-IC_{50} = 0.047 μM) showed enhanced activity compared to AST. However, methylation of the benzimidazole nitrogen (**5d**) led to a 7.5-fold reduction in activity (*Pf*NF54-IC_{50} = 0.35 μM) as compared to **5c** (*Pf*NF54-IC_{50} = 0.047 μM), demonstrating the plausible contribution of the free benzimidazole nitrogen towards the potency of **5c**. Additionally, the antiplasmodium activity of **5c** (*Pf*K1-IC_{50} = 1.7 μM) was ablated in the *Pf*K1 drug-resistant strain

(*Pf*K1-IC_{50} = 1.7 uM), and this compound showed a high propensity for cross-resistance with CQ (RI = 35). Regarding the substituents replacing the 4-fluoro group on the benzyl motif, electron withdrawing substituents such as cyano (**9**; *Pf*NF54-IC_{50} = 0.078 μM), sulfonyl (**14**; *Pf*NF54-IC_{50} = 0.23 μM) and methyl ketone (**15**; *Pf*NF54-IC_{50} = 0.12 μM) were tolerated and showed comparable activity to AST. On the other hand, amide (**13**; *Pf*NF54-IC_{50} = 0.41 μM), acid (**12;** *Pf*NF54-IC_{50} = 1.5 μM) and pyridyl (**16**; *Pf*NF54-IC_{50} = 1.7 μM) replacements reduced potency approximately by five-, seventeen- and nineteen-fold, respectively. The flouro (**7;** *Pf*NF54-IC_{50} = 0.068 μM, and **8;** *Pf*NF54-IC_{50} = 0.075 μM) and two of the cyano (**9;** *Pf*NF54-IC_{50} = 0.078 μM, and **10;** *Pf*NF54-IC_{50} = 0.055 μM) regio-isomers showed comparable activity to AST, while the 2-cyano analogue (**11**; *Pf*NF54-IC_{50} = 0.033 μM) showed more than two-fold enhanced potency compared to AST. This demonstrated that substituent positional change on the benzyl group is tolerated and may deliver compounds with enhanced potency.

Regarding changes to the RHS, the DM-AST congener, **17**, bearing a 4-cyano benzyl group was three-fold more potent than AST (*Pf*NF54-IC_{50} = 0.086 μM) and showed slightly better activity than DM-AST (*Pf*NF54-IC_{50} = 0.04 μM vs 0.028 μM). The methoxy regio-isomers **18** (*Pf*NF54-IC_{50} = 0.089 μM), **19** (*Pf*NF54-IC_{50} = 0.077 μM) and the unsubstituted derivative **20** (*Pf*NF54-IC_{50} = 0.089 μM) were equipotent and had comparable activity to AST.

A selected number of analogues (**5c**, **7-11** and **18-20;** *Pf*NF54-$IC_{50} \leq 0.1$ μM) were advanced for evaluation of cytotoxicity in CHO cells, exhibiting high selectivity indices (selectivity index, SI > 100; **Table 1**). All the analogues except **11** and **15** also exhibited generally good aqueous solubility (**Supplementary Information Table S1**). There was no discernible improvement in solubility among the derivatives relative to AST, except when the benzyl on the LHS of the molecule was replaced with a methyl group (**5d**; 155 μM).

Table 1: Antiplasmodium activity and cytotoxicity of AST and the synthesized analogues.

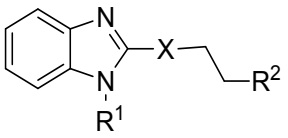

				Antiplasmodium Activity IC_{50} (µM)[a,b]			Cytotoxicity	
							CHO[d] IC_{50}	
Compound	**R^1**	**X**	**R^2**	***Pf*NF54**	***Pf*K1**	**R.I.[c]**	**(µM)**	**S.I.[e]**
AST	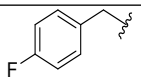	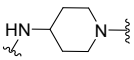	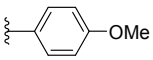	0.086	0.37	4.3	29.6	344
DM-AST	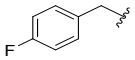	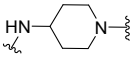	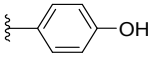	0.040	0.03	0.8	23.0	575
Nor-AST	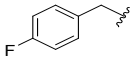	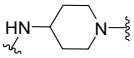	----	1.1	0.92	0.8	--	--
3	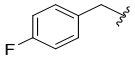	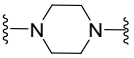	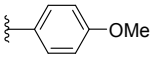	1.9	-	-	--	--
5c	H	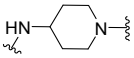	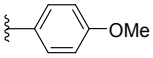	0.047	1.7	36.2	40.4	860
5d		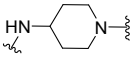	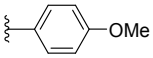	0.35	2.2	6.3	--	--
7	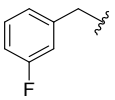	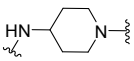	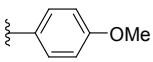	0.068	0.31	4.6	43.8	644
8	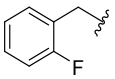	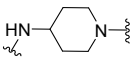	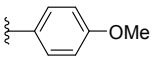	0.075	0.34	4.5	40.4	539
9	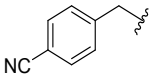	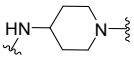	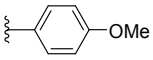	0.078	0.36	4.6	21.2	272
10	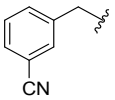	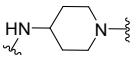	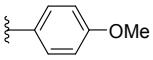	0.055	0.33	6.0	39.7	722
11	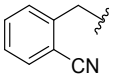	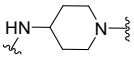	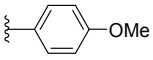	0.033	0.18	5.5	43.6	1321
12	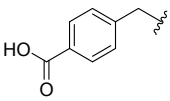	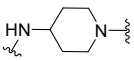	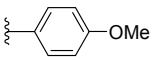	1.5	-	-	--	--

Compound	R^1	X	R^2	Antiplasmodium Activity IC_{50} (µM)[a,b] *Pf*NF54	*Pf*K1	R.I.[c]	Cytotoxicity CHO[d] IC_{50} (µM)	S.I.[e]
13	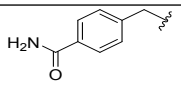	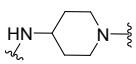	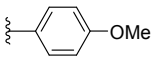	0.41	2.2	5.4	--	--
14	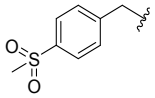	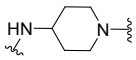	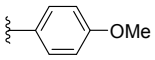	0.23	1.3	5.7	--	--
15	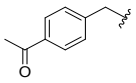	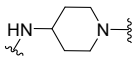	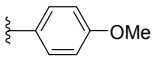	0.12	0.43	3.6	--	--
16	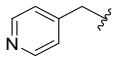	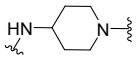	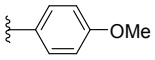	1.7	--	--	--	--
17	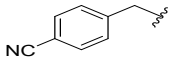	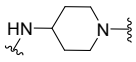	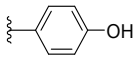	0.028	0.041	1.5	38.5	1376
18	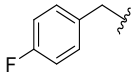	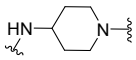	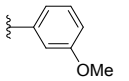	0.089	0.43	4.8	41.0	461
19	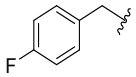	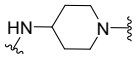		0.077	0.32	4.2	43.1	560
20	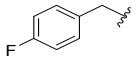	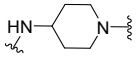		0.086	0.37	4.3	32.4	377
Chloroquine				0.004	0.14	35.0	--	--
Artesunate				0.003	0.001	0.3	--	--
Emetine							0.95	

[a]All the *in vitro* antiplasmodium testing was performed in Modified [^{3}H]-hypoxanthine incorporation assay at Swiss TPH except compounds **16** and **17** which were evaluated in parasite lactate dehydrogenase assay at UCT; [b] Readout is mean from two independent experiments (n = 2) for multidrug resistant (*Pf*K1) and CQ-sensitive (*Pf*NF54) strains of *P. falciparum*; [c]RI = Resistance Index (*Pf*K1-IC_{50}/*Pf*NF54-IC_{50}); [d]CHO = Chinese hamster ovarian cells; [e]SI = Selectivity Index (CHO IC_{50}/*Pf*NF54-IC_{50}).

Gametocyte and Liver Stage Activity: While the ability of AST to inhibit proliferation of *P. berghei* liver stage parasites has been documented,[10] there are no reports on the gametocytocidal potential of this class of compounds. We therefore tested AST, DM-AST and nine other AST analogues (**3, 5c, 10, 11, 14, 15** and **18-20**) against late (LG; > 95% stage IV/V) gametocytes. Only two analogues showed activity, with **5c** (IC_{50} = 1.9 μM) being the most potent against late stage gametocytes compared to AST (IC_{50} = 3.4 μM) and **18** (IC_{50} = 4.1 μM) (**Table 2**). None of the compounds showed improved activity against early stage gametocytes (> 90% stage II/III) compared to AST (data not shown). To the best of our knowledge, this data represents the first evidence of activity of AST and its derivatives against gametocytes.

Table 2: Gametocyte and liver stage activity of AST and analogues:

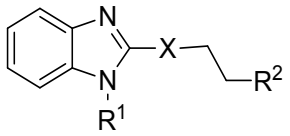

Compound	R^1	X	R^2	IC_{50} (μM)			Cell confluency (% of control)
				[a]Late gametocyte stage	[b]Liver stage	Blood stage	
AST	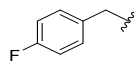	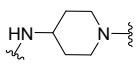	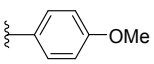	3.4	0.66 ± 0.79	0.086	>73%
DM-AST	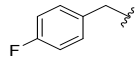	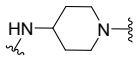	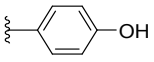	NS[c]	0.14 ± 0.031	0.04	>91%
3	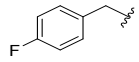	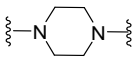	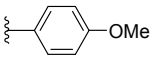	NS[c]	0.21 ± 0.12	1.9	>91%
5c	H	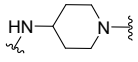	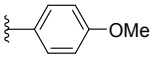	1.9	NS[d]	0.047	NS[d]
18	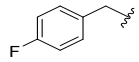	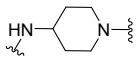		4.1	NS[d]	0.089	NS[d]
Primaquine					8.4		

MB	0.14	
Chloroquine		0.004

[a]Late gametocyte stage: Data was obtained in a single experiment (n = 1) as a technical triplicate; [b]Liver stage: Data represents the mean ± SD of n = 3 independent experiments performed in triplicate obtained for inhibition of the infection of human hepatoma cells (Huh7) by *P berghei*; NS[c]: Not selected for IC_{50} determination as they showed < 50% inhibition in an initial dual-point screen at 1 and 5 μM; NS[d]: Not selected for IC_{50} determination due to < 50% reduction in liver stage parasite load at ≤ 1.0 μM concentration; MB = methylene blue.

The potential for inhibition of liver stage infection was probed using a model of *P. berghei*-infection of the Huh7 human hepatoma cell line.[13] Preliminary screening for liver stage activity of AST, DM-AST, Nor-AST, **3**, **5c**, **7-15** and **17-20** at four different concentrations (10 μM, 1 μM, 0.1 μM and 0.01 μM) showed that only DM-AST and analogue **3** exhibited > 50% reduction of parasite load at ≤ 1 μM with IC_{50} values of 0.14 μM and 0.21 μM, respectively (**Table 2**). In parallel, Huh7 cell confluency was assessed in the presence of each compound concentration, as a measurement of cytotoxicity (Table 2). The activity of AST in our analysis was, however, lower than reported by Derbyshire *et al (*AST: IC_{50} = 0.114 μM),[10] which might result from the fact that different cell lines were employed in two protocols (HepG2 versus HuH7) or from distinct varying cell densities in each assay.[10]

Mechanistic Studies: In humans, AST competitively binds to histamine H_1 receptor sites.[14] Although Chong and colleagues implicated the inhibition of heme crystallization within the parasite in AST's activity, the drug's exact MoA in *Plasmodium* is yet to be established.[5] Employing a pyridine-based, detergent-mediated *in vitro* model that partially recapitulates the micro-environment within the DV and quantifies the inhibition of formation of synthetic Hz, β-

haematin (βH),[15] we assessed the ability of AST derivatives to block βH formation as surrogate for the inhibition of heme detoxification by the parasite. Invoking a discriminatory IC_{50} of 100 μM to identify active inhibitors, four of the twenty evaluated compounds blocked βH formation, albeit less potently than the standard βH formation inhibitors amodiaquine (IC_{50}: 11 μM) and CQ (IC_{50}: 23 μM) (**Supplementary Information Table S1**). Although inhibition was not directly linked to any specific structural modification of AST, all the active derivatives comprised analogues bearing nitrile or carboxylic acid substitution of the fluorine at the C4 position on the LHS phenyl ring. Seeking possible structure-activity relationships, we observed a strong and significant positive correlation (R^2 = 0.6759, p < 0.0001) between βH inhibition and activity against *Pf*NF54 (**Supplementary Information Figure S1**), As a caveat, we reiterate that this assay represents an *in vitro* set-up with the attendant limitations of mimicking the physiological complexities of intracellular drug activity, which include membrane permeation and vacuolar accumulation. These data support inhibition of the heme detoxification pathway as a possible contributing mechanism of the antiplasmodium action of the AST derivatives analysed in the present study.

To establish whether or not this series actually inhibits intracellular Hz formation in *P. falciparum*, DM-AST and compound **10** (with βH inhibitory profiles) were progressed into a cellular heme fractionation assay designed to delineate a dose-dependent effect of compounds on the various heme species (Hb, free heme and Hz) in the parasite.[16] Exposure of synchronized ring stage *Pf*NF54 parasites to each of the two compounds for 32 h led to statistically significant concentration-dependent increases in the proportions of free heme and a corresponding decrease in Hz, similarly to what is observed for CQ (**Figure 3**). Indeed, this concentration-dependent profile persisted for both derivatives when the analysis was focused on the amount of heme (expressed as mass of heme Fe) measured per cell. Thus, these results, corroborate the findings of

Chong et al.,[5] as they strongly suggest that inhibition of Hz formation is a likely, although not necessarily the only, potential MoA of these two AST analogues. Indeed, given the liver stage activity of DM-AST, there must be other targets, suggesting a possible pleiotropic mechanism, at least for this compound.

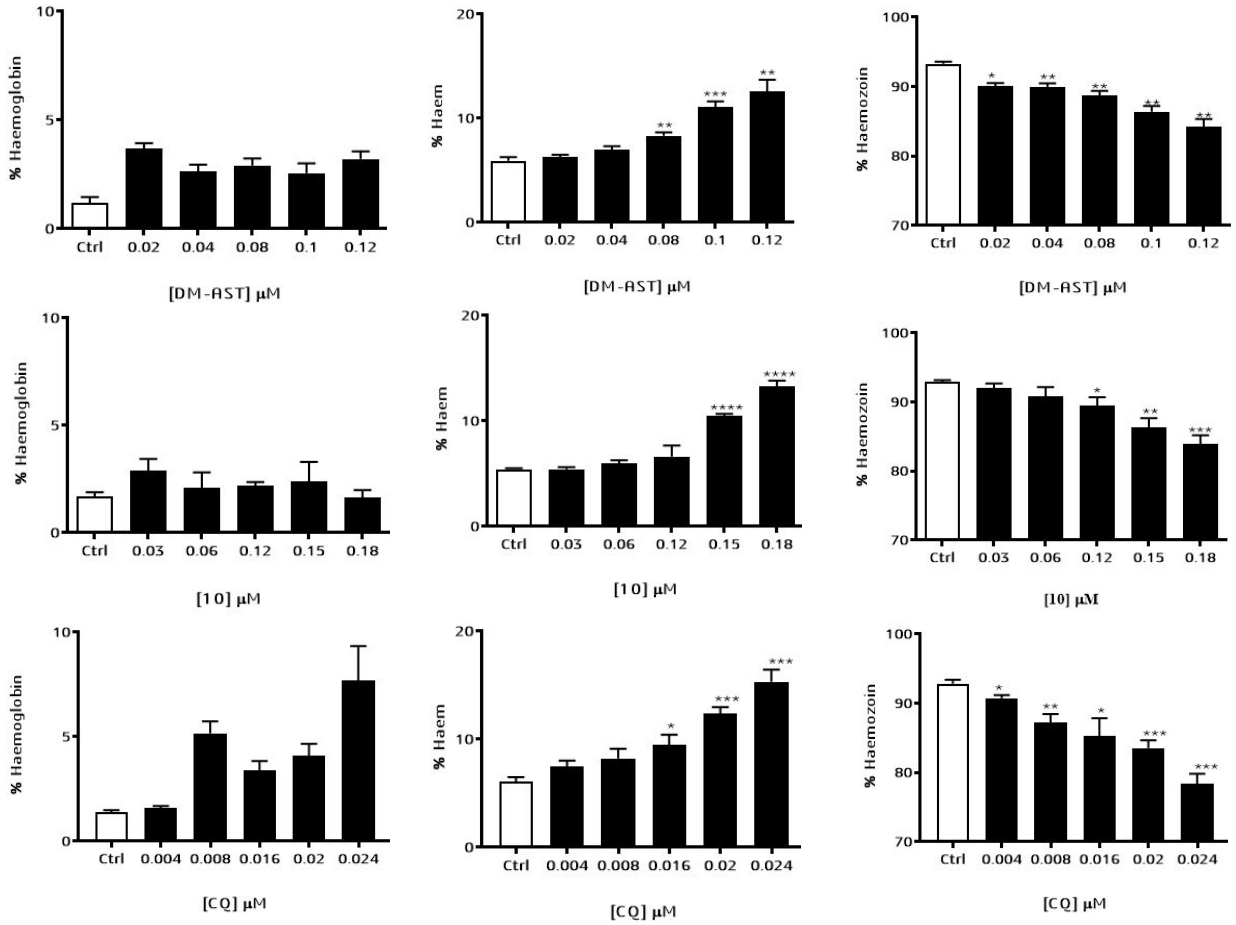

Figure 3: Dose-dependent effect of DM-AST, **10** and CQ on Hb (left panels), 'free' heme (middle panels), and Hz (right) panels in *Pf*NF54. Significant increases in Hb and heme and decreases in Hz relative to the control were calculated using a two-tailed *t*-test and are denoted in asterisk: (∗) $P < 0.05$; (∗∗) $P < 0.01$; (∗∗∗) $P < 0.001$.

CONCLUSION:

As follow up on earlier work on the antimalarial activity of AST, we have presented an investigation on the derivatization and evaluation of the cytotoxicity, activity against different stages of the parasite life cycle, and potential MoA of AST and seventeen analogues. Structural modifications of the AST pharmacophore showed that replacement of the 4-fluoro group on the LHS with a nitrile group was particularly favoured for blood stage activity, especially when accompanied by a hydroxyl substitution for the methoxy group on the RHS of the molecule. Appreciable activity against late stage gametocytes and liver stage parasites was also observed, thus introducing the possibility for optimization towards dual- or triple-action antimalarial agents. To this end, **5c** represents a promising starting point due to its good asexual blood and moderate sexual gametocyte stage activities while further optimization of **3** should be aimed at improving its asexual blood stage activity to match its good liver stage activity. In addition, our data confirm previous findings of the likely contribution of inhibition of heme detoxification as a contributing mechanism to the antiplasmodium effect of AST. Finally, the high selectivity observed for these molecules highlights their cellular safety, at least in lower mammals. Further optimization and evaluation of additional AST derivatives is thus warranted.

EXPERIMENTAL:

All commercially available chemicals were purchased from Sigma-Aldrich or Combi-Blocks, South Africa. All solvents were dried by appropriate techniques. Unless otherwise stated, all solvents used were anhydrous. ^{1}H-NMR and ^{13}C-NMR spectra were recorded on Bruker spectrometer at 400 MHz (^{1}H 400.2 MHz; ^{13}C 100.6 MHz) or Bruker-600 (^{1}H 600.3 MHz; ^{13}C 150.9 MHz). Melting points were determined on a Lasec automatic melting point machine. Analytical thin-layer chromatography (TLC) was performed on aluminium-backed silica-gel 60

F_{254} (70-230 mesh) plates with detection and visualization done using (a) UV lights (254/366 nm), (b) iodine vapor and (c) ninhydrin spray reagent. Column chromatography was performed with Merck silica-gel 60 (70-230 mesh). Chemical shifts (δ) are given in ppm downfield from TMS as the internal standard. Coupling constants were recorded in Hertz (Hz). Purity was determined by Agilent 1260 Infinity binary pump, Agilent 1260 Infinity diode array detector (DAD), Agilent 1290 Infinity column compartment, Agilent 1260 Infinity standard autosampler, and Agilent 6120 quadrupole (single) mass spectrometer, equipped with APCI and ESI multimode ionization source, and all compounds tested for biological activity were confirmed to have ≥ 95% purity. The HPLC method used is described in material and method section. Any data not shown below is supplied in the Supporting files.

1-(4-fluorobenzyl)-2-(piperazin-1-yl)-1H-benzo[d]imidazole (**2**)

A solution **1b** (0.2 grams, 0.071 mmol) and piperazine (0.66 grams, 0.71 mmol) in *t*-BuOH was treated with triethyl amine (0.77 grams, 1.1 mL, 0.71 mmol). The resulting reaction mixture was stirred at 120 °C in a closed vessel for 48 h. After the completion of reaction, reaction was quenched with aqueous saturated solution of $NaHCO_3$ and extracted with ethyl acetate (4 × 10 mL). The combined organic layers were dried over sodium sulfate and concentrated *in vacuo* to afford crude product. The recrystallization of crude product from a mixture of pentane and DCM furnished pure compound **2** (0.2 grams, 87% yield). m.p. 107.9-108.9 °C; ^{1}H-NMR (400 Hz, CD_3OD @ 50 °C): δ_{ppm} 7.53 (d, J = 7.6 Hz, 1H,), 7.25-7.10 (m, H-1, 5H), 7.05 (t, J = 8.4 Hz, 2H), 5.32 (s, 2H), 3.27 (t, J = 5.2 Hz, 4H), 3.04 (t, J = 4.8 Hz, 4H); ^{13}C-NMR (101 Hz, MeOD @ 50 °C) δ_{ppm} 162.29 (d, J = 244.9 Hz, C-F), 157.7, 140.7, 134.7, 132.41 (d, J = 3.0 Hz), 128.10 (d, J = 8.1 Hz, 2C), 122.0, 121.7, 117.1, 115.23 (d, J = 21.9 Hz, 2C), 109.6, 50.4 (2C), 46.4 and 44.4 (2C); LC-MS (APCI/ESI)$^+$: *m/z* $[M+H]^+$ = 311.2 (calculated for $C_{18}H_{19}FN_4$, 310.16).

1-(4-fluorobenzyl)-2-(4-(4-methoxyphenethyl)piperazin-1-yl)-1H-benzo[d]imidazole (3)

A solution of **2** (0.15 grams, 0.48 mmol), 1-(2-bromoethyl)-4-methoxybenzene (0.21 grams, 0.151 mL, 0.57 mmol) and triethyl amine (0.12 grams, 0.17 mL, 0.12 mmol) in toluene was refluxed (110 °C) for 48 h. After the completion of reaction, concentrated *in vacuo* and residue was dissolved in ethyl acetate (20 mL). This mixture was washed with sat. $NaHCO_3$ (2 × 15 mL), dried over sodium sulfate and concentrated *in vacuo*. Purification of residue by biotage flash chromatography at 5% MeOH: DCM and recrystallization from a mixture of pentane and DCM provided **3** as a white solid (0.12 grams, 50%); ^{1}H-NMR (400 Hz, CD_3OD @ 50 °C): δ_{ppm} 7.53 (d, J = 8.0 Hz, 1H), 7.23-7.12 (m, 6H), 7.13-7.09 (m, 1H), 7.08-7.03 (m, 2H), 6.84 (d, J = 8.8 Hz, 2H), 5.31 (s, 2H), 3.77 (s, 3H), 3.35-329 (m, 4H), 2.81-2.75 (m, 2H), 2.69 (m, 4H), 2.67-2.61 (m, 2H); ^{13}C-NMR (101 Hz, MeOD @ 50 °C) δ_{ppm} 162.31 (d, J = 244.9 Hz, C-F), 158.3, 157.8, 140.8, 134.8, 132..46 (d, J = 2.7 Hz), 132.0, 129.2 (2C), 128.08 (d, J = 8.2 Hz, 2C), 121.9, 121.6, 117.0, 115.23 (d, J = 21.9, 2C), 113.6 (2C), 109.5. 60.2, 54.4, 52.4 (2C), 50.1 (2C), 46.5 and 31.8; LC-MS (APCI/ESI)$^+$, found m/z = 445.2 $[M+H]^+$ (calculated for $C_{27}H_{29}FN_4O$, 444.23); Purity = 99.9% (t_r = 4.035 min).

Synthesis of 4-*N*-Boc-((1H-benzo[d]imidazol-2-yl) amino) piperidine (5a). A mixture of 2-chlorobenzimidazole (**1a**) (2.0 grams, 13.2 mmol) and 4-amino-N-Boc-piperidine (3.15 grams, 15.7 mmol) in TEA (5.50 mL, 39.4 mmol) where stirred under a nitrogen atmosphere at 150 °C for 2 h. After the completion of reaction, dissolved in DCM (25 mL) followed by washing with $NaHCO_3$ (2 × 20 mL), brine (2 × 20 mL), dried over anhydrous Na_2SO_4 and concentrated *in vacuo*. Residue was washed with EtOAc to obtained **5a** as a white solid (2.49 grams, 60%). ^{1}H-NMR (300 MHz, DMSO-d6) δ 10.59 (s, 1H), 7.12 (t, J = 6.9 Hz, 2H), 6.86 (dt, J = 12.4 and 7.2 Hz, 2H), 6.50 (d, J = 8.0 Hz, 1H), 3.90 (d, J = 13.3 Hz, 2H), 3.83 – 3.68 (m, 1H), 2.87 (d, J = 13.5 Hz, 2H), 1.93

(dd, J = 12.6 and 3.7 Hz, 2H), 1.41 (s, 9H), 1.39 – 1.27 (m, 2H). LC-MS (APCI/ESI)$^+$, found m/z = 317.1 $[M+H]^+$ (cal. for $C_{17}H_{24}N_4O_2$, 316.19).

Ethyl 4-((1-(4-fluorobenzyl)-1H-benzo[d]imidazol-2-yl)amino)piperidine-1-carboxylate (5b)

A neat mixture of **1b** (1.5 grams, 5.75 mmol) and ethyl 4-aminopiperidine-1-carboxylate (2.0 grams, 11.62 mmol) was heated to 170 °C and stirred for 4 h. After completion of the reaction, it was cooled to ambient temperature (23 °C), dissolved in DCM (50 mL), washed with saturated $NaHCO_3$ (2 × 20 mL), dried over sodium sulfate and concentrated *in vacuo*. Purification by column chromatography using 0.2-1% MeOH: DCM afforded **5b** as a white solid (2.3 grams, 98% yield); m.p. 175.8-178.7 °C; ^{1}H-NMR (400 Hz, $CDCl_3$): δ_{ppm} 7.55 (d, J = 8.0 Hz, 1H), 7.22-7.11 (m, H-1, 3H), 7.10-7.00 (m, 4H), 5.14 (s, 2H), 4.22-3.90 (m, 3H), 4.11 (q, J = 8.0 Hz, 2H), 4.24 (q, J = 8.0 Hz, 2H), 2.10 (m, 2H), 1.33 (m, 2H) and 1.25 (t, J = 8.0 Hz, 3H); LC-MS (APCI/ESI)$^+$, found m/z = 397.2 $[M+H]^+$ (calculated for $C_{22}H_{25}FN_4O_2$, 396.20).

***N*-(1-(4-methoxyphenethyl)piperidin-4-yl)-1H-benzo[d]imidazol-2-amine (5c)**

A neat mixture of **1a** (0.1 grams, 0.657 mmol) and 1-(4-methoxyphenethyl)piperidin-4-amine (0.31 grams, 1.323 mmol) was heated to 170 °C and stirred for 4 h. After completion of the reaction, the reaction mixture was cooled down to ambient temperature (23 °C), dissolved in DCM (20 mL), washed with sat. $NaHCO_3$ (2 × 10 mL), dried over sodium sulfate and concentrated *in vacuo*. Purification by column chromatography using 0-1% MeOH: DCM afforded **5c** as a white solid (0.11 grams, 48% yield). ^{1}H-NMR (Methanol-d_4, 400 MHz) δ 7.24-7.17 (m, 2H), 7.13 (d, J = 8.8 Hz, 2H), 700-6.94 (m, 2H), 6.85 (d, J = 8.4 Hz, 2H), 3.76 (s, 3H), 3.72-3.62 (m, 1H), 3.10-2.96 (m, 2H), 2.82-2.71 (m, 2H), 2.64-2.54 (m, 2H), 2.29 (t, J = 9.2 Hz, 2H), 2.15-2.10 (m, 2H), 1.71-1.54 (m, 2H); ^{13}C-NMR (101 MHz, MeOD) δ 158.7, 154.3, 137.6, 131.7, 129.2 (2C), 119.9,

113.6 (2C), 111.3 (4C), 60.3, 54.3, 52.0 (2C), 49.3, 32.0 and 31.7 (2C); LC-MS (APCI/ESI)$^+$, found *m/z* = 351.2 $[M+H]^+$ (calculated for $C_{21}H_{26}N_4O$, 350.2), Purity = 97.1% (t_r = 0.197 min).

4-((2-((1-(4-methoxyphenethyl)piperidin-4-yl)amino)-1H-benzo[d]imidazol-1-yl)methyl)benzonitrile (5d)

A solution of **1a** (0.3 grams, 1.967 mmol) and methyl iodide (1.5 grams, 10.709 mmol) in DMF (3 mL) was charged with potassium carbonate (2.95 grams, 19.67 mmol). The resulting reaction mixture was stirred at room temperature (23 °C) for 30 mins. After the completion of reaction, quenched with water (10 mL), extracted with ethyl acetate (5 × 10 mL), dried over sodium sulphate and concentrated to obtain the crude product (0.225 grams, 68% yield), which was washed with *n*-pentane and used in next step without further purification.

A neat mixture of methylated product from previous step (0.075 grams, 0.450 mmol) and 1-(4-methoxyphenethyl)piperidin-4-amine (0.2 grams, 0.90 mmol) was heated to 170 °C and stirred for 8 h. After the completion of the reaction, it was cooled to ambient temperature (23 °C), dissolved in DCM (20 mL), washed with sat. $NaHCO_3$ (2 × 10 mL), dried over sodium sulfate and concentrated *in vacuo*. Purification by column chromatography using 0-1% MeOH: DCM afforded **5d** as a yellow solid (0.055 grams, 30% yield). ^{1}H-NMR (Methanol-d_4, 400 MHz) δ 7.33-7.27 (m, 1H), 7.21-7.11 (m, *J* = 8.4 Hz, 3H), 7.10-7.0 (m, 2H), 6.87 (d, *J* = 8.0 Hz, 2H), 3.88-3.80 (m, 1H), 3.76 (s, 3H), 3.55 (s, 3H), 3.21-3.11 (m, 2H), 2.87-2.76 (m, 2H), 2.74-2.65 (m, 2H), 2.39 (t, *J* = 9.2 Hz, 2H), 2.21-2.12 (m, 2H), 1.80-1.66 (m, 2H); ^{13}C-NMR (101 MHz, MeOD) δ 158.4, 154.2,

141.2, 134.6, 131.4, 129.2 (2C), 120.7, 119.3, 114.4, 113.6 (2C), 107.0, 60.1, 54.3, 52.3 (2C), 49.7, 31.7, 31.2 (2C) and 27.2; LC-MS (APCI/ESI)$^+$, found *m/z* = 365.2 $[M+H]^+$ (calculated for $C_{22}H_{28}N_4O$, 364.2), Purity = 95.5% (t_r = 0.200 min).

4-((2-(piperidin-4-ylamino)-1H-benzo[d]imidazol-1-yl)methyl)benzonitrile (6a).

A mixture of **5a** (2.20 grams, 6.96 mmol), 4-(bromomethyl) benzonitrile (1.64 grams, 8.4 mmol) and K_2CO_3 (2.40 grams, 17.4 mmol) in DMF (9 mL) was stirred under a nitrogen atmosphere at 70 ^oC for 3 h. After the completion of the reaction, it was cooled to ambient temperature (23 °C) and diluted with EtOAc (50 mL). The resulting mixture was washed with water (3 × 30 mL), 5% LiCl (20 mL × 2) and brine (20 mL × 2), dried over sodium sulfate and concentrated *in vacuo*. The residue was washed with diethyl ether and used in next step without further purification.

A suspension of *N*-Boc protected compound from the previous step in 4N HCl in dioxane (1 mL per 0.100 grams) was stirred at ambient temperature (20 °C) for 2 h. After the completion of reaction, dioxane was removed under vacuum and residue was taken in EtOAc (25 mL) and neutralized with 15% NaOH pH > 8) while stirring in an ice bath. The organic phase was dried over anhydrous Na_2SO_4 and evaporated under vacuum to afford **6a** (2.50 grams, 5.80 mmol, 1 eq) as a pale yellow solid (1.54 grams, 80% yield). ^{1}H-NMR (300 MHz, Methanol-d_4) δ 7.70 – 7.64 (m, 2H), 7.32 (dt, *J* = 7.8, 0.9 Hz, 1H), 7.28 – 7.22 (m, 2H), 7.05 (ddd, *J* = 7.9, 6.9, 1.7 Hz, 1H), 6.99 (ddd, *J* = 7.9, 1.7, 0.7 Hz, 1H), 6.94 (ddd, *J* = 7.9, 6.9, 1.1 Hz, 1H), 5.37 (s, 2H), 3.89 (tt, *J* = 11.1, 4.1 Hz, 1H), 3.07 (dt, *J* = 12.9, 3.5 Hz, 2H), 2.74 (td, *J* = 12.5, 2.6 Hz, 2H), 2.06 (dd, *J* = 12.7, 3.7 Hz, 2H), 1.46 (qd, *J* = 11.9, 4.1 Hz, 2H). ^{13}C-NMR (101 MHz, Methanol-d_4) δ 153.95,

142.34, 141.70, 133.89, 132.25, 127.13, 121.29, 119.54, 118.05, 114.85, 111.02, 107.51, 50.16, 44.66, 44.23, 32.45. LC-MS (APCI/ESI): found *m/z* = 331.9 $[M+H]^+$ (cal. for $C_{20}H_{21}N_5$, 331.18).

1-(4-fluorobenzyl)-N-(piperidin-4-yl)-1H-benzo[d]imidazol-2-amine (Nor-AST)

A solution of **5b** (2.3 grams, 5.80 mmol) in HBr (48%, 17 mL) was refluxed (120 °C) for 3 h. After completion of the reaction, it was cooled to 0 °C and treated with 2.5 M aqueous NaOH in dropwise manner to neutralized excess of HBr (pH = 12-14). The extraction of organic compounds was done with chloroform (5 × 20 mL). The combined organic layers were dried over sodium sulfate and concentrated *in vacuo* to obtain Nor-AST as an orange solid (1.89 grams, 85% yield); ^{1}H-NMR (400 Hz, $CDCl_3$): δ_{ppm} 7.52 (d, *J* = 8.0 Hz, 1H), 7.19-7.08 (m, 3H), 7.07-6.98 (m, 4H), 5.07 (s, 2H), 3.04 (dt, *J* = 12.4 and 4.8 Hz, 2H), 2.75 (td, *J* = 12.0 and 2.8 Hz, 2H), 2.41 (bs, 1H), 2.10 (m, 2H) and 1.32 (m, 2H); ^{13}C-NMR (101 Hz, $CDCl_3$): δ_{ppm} 162.44 (d, *J* = 247.3 Hz, C-F), 153.3, 142.4, 134.5, 131.19 (d, *J* = 3.3 Hz), 128.22 (d, *J* = 8.3 Hz, 2C), 121.5, 119.8, 116.6, 116.13 (d, *J* = 21.8 Hz, 2C), 107.2, 50.2, 45.2 (2C), 45.0 and 33.8 (2C); LC-MS $(APCI/ESI)^+$, found *m/z* = 325.2 $[M+H]^+$ (calculated for $C_{19}H_{21}FN_4$, 324.18), Purity = 95.2% (t_r = 2.819 min).

General procedure 1 for the synthesis of AST and compounds 7-16: A solution of 2-chloro-1H-benzo[d]imidazole (1 equivalent) in acetone was charged with K_2CO_3 (2.5 equivalent) and respective benzyl bromide (1.5 equivalent). The resulting reaction mixture was stirred at room temperature (23 °C) for 4-6 hours. After completion of the reaction, it was filtered and concentrated. The crude product was washed with *n*-pentane to obtain **4** and used in next step without further purification.

A mixture of respective benzylated benzimidazole intermediate **4** (1 equivalents) and 1-(4-methoxyphenethyl)piperidin-4-amine (2 equivalents) was heated to 170 °C and stirred for 6-12 h.

After the completion of reaction, cooled to ambient temperature (23 °C) and resulting solid was dissolved in DCM, washed with saturated solution of sodium bicarbonate (twice), water (twice) and brine. The organic phase was dried over sodium sulphate and concentrated *in vacuo* to obtain crude product, which was purified by column chromatography using 1-10% MeOH: DCM to afford pure compounds.

1-(4-fluorobenzyl)-N-(1-(4-methoxyphenethyl)piperidin-4-yl)-1H-benzo[d]imidazol-2-amine (AST)

White solid (72% yield); ^{1}H-NMR (400 Hz, CD_3OD): δ_{ppm} 7.32 (d, J = 8.0 Hz, 1H), 7.19-7.10 (m, 4H), 7.08-7.00 (m, 4H), 6.95 (td, J = 8.0 and 0.8 Hz, 1H) 6.84 (dd, J = 8.8 and 2.4 Hz, 2H), 5.25 (s, 2H), 3.84 (tt, J = 12.0 and 4.0 Hz, 1H), 3.76 (s, 3H), 3.01 (m, 2H), 2.76 (m, 2), 2.58 (m, 2H), 2.27 (m, 2H), 2.09 (m, 2H), 1.69-1.53 (m, 2H); ^{13}C-NMR (101 Hz, CD_3OD): δ 162.19 (d, J = 242.4 Hz), 158.2, 154.0, 141.7, 134.0, 132.4 (d, J = 2.02 Hz) , 131.8, 129.2 (2C), 128.23 (d, J = 8.1 Hz; 2C), 121.1, 119.4, 115.06 (d, J = 21.8 Hz, 2C), 114.7, 113.6 (2C), 107.7, 60.4, 54.3, 52.2, 49.9, 43.9, 32.0 and 31.5; LC-MS (APCI/ESI)$^{+}$, found *m/z* = 459.2 $[M+H]^{+}$ (calculated for $C_{28}H_{31}FN_4O$, 458.25); Purity = 95.7%, (t_r = 3.525 min).

1-(3-fluorobenzyl)-N-(1-(4-methoxyphenethyl)piperidin-4-yl)-1H-benzo[d]imidazol-2-amine (7)

White solid (70%);^{1}H-NMR (Methanol-d_4, 400 MHz) δ 7.37-7.28 (m, 2H), 7.18-7.12 (d, J = 8.8 Hz, 2H), 7.09-7.01 (m, 2H), 7.0-6.91 (m, 2H), 6.98-6.80 (m, 2H), 5.31 (s, 2H), 3.86 (tt, J = 12.0 and 4.0 Hz, 1H), 3.77 (s, 3H), 3.10-2.95 (m, 2H), 2.83-2.70 (m, 2H), 2.66-2.52 (m, 2H), 2.29 (td, J = 9.2 and 2.0 Hz, 2H), 2.15-2.05 (m, 2H), 1.72-1.59 (m, 2H); ^{13}C-NMR (101 MHz, MeOD) δ 163.09 (d, J = 245.3 Hz, C-F), 158.2, 154.0, 141.6, 139.45 (d, J = 6.98 Hz), 134.0, 131.8, 130.25 (d, J = 8.27 Hz), 129.2 (2C), 122.0, 121.1, 119.5, 114.7, 113.89 (d, J =21.3 Hz), 113.6 (2C), 113.07

(d, J = 22.6 Hz), 107.6, 60.4, 54.3, 52.3 (2C), 49.9, 44.0, 31.9, 31.3 (2C); LC-MS (APCI/ESI)$^+$, found m/z = 459.1 $[M+H]^+$ (calculated for $C_{28}H_{31}FN_4O$, 458.25); Purity = 97.8%, (t_r = 3.989 min).

1-(2-fluorobenzyl)-N-(1-(4-methoxyphenethyl)piperidin-4-yl)-1H-benzo[d]imidazol-2-amine (8)

White solid (64%); ^{1}H-NMR (Methanol-d_4, 400 MHz) δ 7.35-7.32 (m, 1H), 7.31-7.36 (m, 1H,), 7.18-7.11 (m, 3H), 7.09-7.00 (m, 3H), 6.95 (ddd, J = 8.4, 7.2 and 1.2 Hz), 6.89-6.81 (m, 3H), 5.34 (s, 2H), 3.86 (tt, J = 12.0 and 4.0 Hz, 1H), 3.78 (s, 3H), 3.09-3.0 (m, 2H), 2.83-2.71 (m, 2H), 2.64-2.54 (m, 2H), 2.30 (td, J = 12 and 3.6 Hz, 2H), 2.16-2.05 (m, 2H), 1.69-1.53 (m, 2H); ^{13}C-NMR (101 MHz, MeOD) δ 160.56 (d, J = 245.2 Hz, C-F), 158.2, 154.1, 141.7, 133.9, 131.9, 129.2 (2C), 128.8, 127.9 (d, J = 3.7 Hz), 124.2, 123.34 (d, J = 14.7 Hz), 121.1, 119.4, 115.03 (d, J = 21.2 Hz), 114.9, 114.7, 113.6 (2C), 107.5, 60.4, 54.3, 52.2 (2C), 50.0, 39.0, 31.9 and 31.2 (2C); LC-MS (APCI/ESI)$^+$, found m/z = 459.1 $[M+H]^+$ (calculated for $C_{28}H_{31}FN_4O$, 458.25); Purity = 99.2%, (t_r = 3.886 min).

4-((2-((1-(4-methoxyphenethyl)piperidin-4-yl)amino)-1H-benzo[d]imidazol-1-yl)methyl)benzonitrile (9)

Pink solid (40%); ^{1}H-NMR (Methanol-d_4, 400 MHz) δ 7.69 (d, J = 8.4 Hz, 2H), 7.36 (d, J = 8.0 Hz, 1H), 7.27 (d, J = 8.4 Hz, 2H), 7.15 (d, J = 8.4 Hz, 2H), 7.08 (t, J = 7.4 Hz, 1H), 7.05 - 7.0(m, 1H), 7.0 - 6.95 (m, 1H), 6.86 (d, J = 8.4 Hz, 2H), 5.40 (s, 2H), 3.94-3.83 (m, 1H), 3.77 (s, 3H), 3.22-3.07 (m, 2H), 2.88-2.77 (m, 2H), 2.77-2.66 (m, 2H), 2.45 (t, J = 12.4 Hz, 2H), 2.21-2.10 (m, 2H), 1.78-1.61 (m, 2H); ^{13}C-NMR (101 MHz, MeOD) δ 158.4, 153.9, 142.3, 141.6, 132.3 (2C), 131.1, 129.2 (3C), 127.1 (2C), 121.4, 119.7, 118.0, 114.9, 113.7 (2C), 111.0, 107.6, 59.9, 54.3,

52.0 (2C), 49.7, 44.3, 31.4, and 31.0 (2C); LC-MS (APCI/ESI)$^+$, found *m/z* = 466.2. $[M+H]^+$ (calculated for $C_{29}H_{31}N_5O$, 465.25); Purity = 99.9%, (t_r = 1.974 min).

3-((2-((1-(4-methoxyphenethyl)piperidin-4-yl)amino)-1H-benzo[d]imidazol-1-yl)methyl)benzonitrile (10)

White solid (15%); ^{1}H-NMR (Methanol-d_4, 400 MHz) δ 7.68-7.67 (m, 1H), 7.55-7.45 (m, 2H), 7.43-7.33 (m, 2H), 7.14 (d, *J* = 7.8 Hz, 2H), 7.11-7.01 (m, 2H), 7.03-6.95 (m, 1H), 6.85 (d, *J* = 8.0 Hz, 2H), 5.35 (s, 2H), 3.98-3.83 (m, 1H), 3.77 (s, 3H), 3.20-3.07 (m, 2H), 2.87-2.77 (m, 2H), 2.76-2.66 (m, 2H), 2.43 (t, *J* = 12.0 Hz, 2H), 2.21-2.09 (m, 2H), 1.80-1.60 (m, 2H); ^{13}C-NMR (101 MHz, MeOD) δ 158.4, 154.0, 141.7, 138.4, 133.9, 131.6, 131.0 (2C), 129.9, 129.6, 129.2 (2C), 127.4, 119.7, 118.0, 115.0, 113.8 (2C), 112.6, 107.6, 59.9, 54.3, 52.1 (2C), 49.8, 44.0, 31.7, and 31.2 (2C); LC-MS (APCI/ESI)$^+$, found *m/z* = 466.2. $[M+H]^+$ (calculated for $C_{29}H_{31}N_5O$, 465.25); Purity = 98.9%, (t_r = 1.977 min).

2-((2-((1-(4-methoxyphenethyl)piperidin-4-yl)amino)-1H-benzo[d]imidazol-1-yl)methyl)benzonitrile (11)

White solid (30%); ^{1}H-NMR (Methanol-d_4, 400 MHz) δ 7.80 (dd, *J* = 6.8 and 0.96 Hz, 1H), 7.52 (td, *J* = 7.60 and 1.2 Hz, 1H), 7.44 (td, *J* = 7.60 and 0.8 Hz, 1H), 7.36 (d, *J* = 7.60 Hz, 1H), 7.14 (d, *J* = 8.4 Hz, 2H), 7.08 (ddd, *J* = 8.4, 6.0 and 2.4 Hz, 1H), 6.98-6.90 (m, 2H), 6.88-6.77 (m, *J* = 8.4 Hz, 3H), 5.52 (s, 2H), 3.95-3.82 (m, 1H), 3.77 (s, 3H), 3.14-3.02 (m, 2H), 2.81-2.74 (m, 2H), 2.68-2.59 (m, 2H), 2.34 (t, *J* = 12.0 Hz, 2H), 2.19-2.09 (m, 2H), 1.75-1.61 (m, 2H); ^{13}C-NMR (101 MHz, MeOD) δ 158.3, 154.1, 141.7, 141.0, 133.9, 131.6, 131.1, 131.5, 129.2 (2C), 127.9, 126.2, 121.4, 119.6, 116.2, 114.9, 113.6 (2C), 110.7, 107.5, 60.2, 54.3, 52.2 (2C), 49.9, 43.3, 31.8, and

31.3 (2C); LC-MS (APCI/ESI)$^+$, found *m/z* = 466.2. $[M+H]^+$ (calculated for $C_{29}H_{31}N_5O$, 465.25); Purity = 99.01% (t_r = 2.027 min).

4-((2-((1-(4-methoxyphenethyl)piperidin-4-yl)amino)-1H-benzo[d]imidazol-1-yl)methyl)benzoic acid (12)

White solid (15%); ^{1}H-NMR (DMSO-d_6, 400 MHz @ 80 ˚C) δ 10.74 (s, 1H), 8.04 (s, 1H), 7.82 (d, *J* = 8.2Hz), 7.38 (d, *J* = 8.3 Hz), 7.16 (d, *J* = 8.6 Hz, 2H), 7.03-6.91 (m, 4H), 6.87 (d, *J* = 8.6 Hz, 2H), 5.04 (s, 2H), 3.97-3.82 (m, 1H), 3.06-2.92 (m, 2H; overlapping with DMSO water peak), 2.89-2.72 (m, 6H), 1.96-1.86 (m, 2H), 1.81-1.65 (m, 2H); ^{13}C-NMR (101 MHz, DMSO-d_6) ^{13}C NMR (101 MHz, DMSO) δ 166.1, 158.3, 154.8, 140.7, 134.3, 130.5, 130.3, 130.1 (2C), 128.8, 128.1 (2C), 127.6 (2C), 121.6, 121.0, 114.3 (2C), 109.4, 108.5, 55.5 (2C), 51.9 (2C), 50.5, 49.9, 49.6 and 43.33 (2C); LC-MS (APCI/ESI)$^+$, found *m/z* = 485.2 $[M+H]^+$ (calculated for $C_{29}H_{32}N_4O_3$, 458.25); Purity = 97.0%, (t_r = 3.989 min).

4-((2-((1-(4-methoxyphenethyl)piperidin-4-yl)amino)-1H-benzo[d]imidazol-1-yl)methyl)benzamide (13)

White solid (29%); ^{1}H-NMR (Methanol-d_4, 400 MHz) δ 7.82 (d, *J* = 8.4 Hz, 2H), 7.35 (d, *J* = 7.8 Hz, 1H), 7.20 (d, *J* = 6.8 Hz, 2H), 7.13 (d, *J* = 8.6 Hz, 2H), 7.11-7.01(m, 2H), 6.99-6.91 (m, 1H), 6.85 (d, *J* = 8.4 Hz, 2H), 5.37 (s, 2H), 3.90-3.80 (m, 1H), 3.77 (s, 3H), 3.08-2.94 (m, 2H), 2.81-2.71 (m, 2H), 2.63-2.53 (m, 2H), 2.28 (t, *J* = 12.0 Hz, 2H), 2.14-2.04 (m, 2H), 1.72-1.56 (m, 2H); ^{13}C-NMR (101 MHz, MeOD) δ 170.4, 158.2, 154.1, 141.7, 140.6, 134.0, 132.9, 131.8, 129.2 (2C), 127.7 (2C), 126.3 (2C), 121.1, 119.4, 114.7, 113.6 (2C), 107.6, 60.4, 54.2, 52.2 (2C), 49.9, 44.3,

31.9, and 31.4 (2C); LC-MS (APCI/ESI)$^+$, found *m/z* = 483.9 $[M+H]^+$ (calculated for $C_{29}H_{33}N_5O_2$, 483.9); Purity = 95.81% (t_r = 2.264 min).

N-(1-(4-methoxyphenethyl)piperidin-4-yl)-1-(4-(methylsulfonyl)benzyl)-1H-benzo[d]imidazol-2-amine (14)

White solid (38%); ^{1}H-NMR (Methanol-d_4, 400 MHz) δ 7.88 (d, *J* = 8.4 Hz, 2H), 7.42-7.31 (m, 3H), 7.13 (d, *J* = 8.6 Hz, 2H), 7.07 (td, *J* = 6.9 and 1.2 Hz, 1H), 7.03-6.99 (m, 1H), 6.99-6.91 (m, 1H), 6.85 (d, *J* = 8.4 Hz, 2H), 5.37 (s, 2H), 3.90-3.80 (m, 1H), 3.77 (s, 3H), 3.06 (s, 3H), 3.04-2.94 (m, 2H), 2.81-2.71 (m, 2H), 2.63-2.53 (m, 2H), 2.28 (t, *J* = 12.0 Hz, 2H), 2.14-2.04 (m, 2H), 1.72-1.56 (m, 2H); ^{13}C-NMR (101 MHz, MeOD) δ ^{13}C-NMR (101 MHz, MeOD) δ 158.3, 154.1, 143.0, 141.8, 140.1, 134.0, 132.0, 129.2 (2C), 127.4, 127.3 (2C), 121.3, 119.6, 115.0, 113.7 (2C), 107.6, 102.1, 60.1, 54.4, 52.1 (2C), 50.0, 44.3, 43.0, 31.9, 31.4 (2C); LC-MS (APCI/ESI)$^+$, found *m/z* = 519.2 $[M+H]^+$ (calculated for $C_{29}H_{34}N_4O_3$, 518.68); Purity = 98.49% (t_r = 1.991 min).

1-(4-((2-((1-(4-methoxyphenethyl)piperidin-4-yl)amino)-1H-benzo[d]imidazol-1-yl)methyl)phenyl)ethan-1-one (15)

White solid (30%); ^{1}H-NMR (Methanol-d_4, 400 MHz) δ 7.92 (d, *J* = 8.0 Hz, 2H), 7.35 (d, *J* = 8.0 Hz, 1H), 7.22 (d, *J* = 8.4 Hz, 2H), 7.13 (d, *J* = 8.6 Hz, 2H), 7.07(td, *J* = 8 and 1.2 Hz, 1H), 7.03-6.99 (m, 1H), 6.99-6.92 (m, 1H), 6.84 (d, *J* = 8.4 Hz, 2H), 5.36 (s, 2H), 3.92-3.82 (m, 1H), 3.76 (s, 3H), 3.15-2.99 (m, 2H), 2.81-2.71 (2H, m), 2.68-2.58 (m, 2H), 2.37 (t, *J* = 12.0 Hz, 2H), 2.19-2.07 (m, 2H), 1.77-1.60 (m, 2H); ^{13}C-NMR (101 MHz, MeOD) δ 198.5, 158.3, 154.0, 142.1, 141.6, 136.2, 134.0, 131.4, 129.2 (2C), 128.5 (2C), 126.5 (2C), 121.2, 119.5, 114.8, 113.6 (2C), 107.7,

60.1, 54.3, 52.1 (2C), 49.7, 44.4, 31.6, 31.1 (2C) and 25.3; LC-MS (APCI/ESI)$^+$, found *m/z* = 483.2 $[M+H]^+$ (calculated for $C_{30}H_{34}N_4O_2$, 482.27); Purity = 95.54% (t_r = 2.147 min).

N-(1-(4-methoxyphenethyl)piperidin-4-yl)-1-(pyridin-3-ylmethyl)-1H-benzo[d]imidazol-2-amine (16)

Yellow solid (36%);^{1}H-NMR (Methanol-d_4, 400 MHz) δ 8.47 (d, *J* = 8.4 Hz, 2H), 7.36 (d, *J* = 7.60 Hz, 1H), 7.17-7.11 (m, 4H), 7.11-7.06 (m, 1H), 7.05-6.99 (m, 2H), 6.86 (d, *J* = 8.4 Hz, 2H), 5.39 (s, 2H), 3.93-3.81 (m, 1H), 3.78 (s, 3H), 3.11-3.03 (m, 2H), 2.84-2.72 (m, 2H), 2.66-2.56 (m, 2H), 2.32 (t, *J* = 12.0 Hz, 2H), 2.15-2.08 (m, 2H), 1.72-1.60 (m, 2H); ^{13}C-NMR (101 MHz, MeOD) δ 158.4, 153.9, 149.0 (2C), 147.2, 141.5, 133.9, 130.8, 129.2 (2C), 121.8, 121.4, 119.7, 116.4, 114.9, 113.7 (2C), 107.5, 59.7, 54.3, 52.0 (2C), 49.4, 43.6, 31.3 (2C) and 30.8; LC-MS (APCI/ESI)$^+$, found *m/z* = 442.2. $[M+H]^+$ (calculated for $C_{27}H_{31}N_5O$, 441.25); Purity = 96.1% (t_r = 1.916 min).

General procedure 2 for the synthesis of 17-20: A solution of *Nor*-AST (1 equivalent) and respective phenylethylbromide (1.3 equivalents) in acetonitrile was charged with K_2CO_3 (2.5 equivalents). The resulting reaction mixture was refluxed for 5-24 hours. After completion of the reaction, it was filtered and concentrated *in vacuo*. The residue was dissolved in DCM and washed with $NaHCO_3$ (2 ×) and brine (2 ×), dried over anhydrous sodium sulphate and concentrated *in vacuo*. The crude product was purified by column chromatography using 0 – 10% MeOH/DCM.

4-((2-((1-(4-hydroxyphenethyl)piperidin-4-yl)amino)-1-benzimidazyl)methyl)benzonitrile (17)

Yellow solid (63%); ^{1}H-NMR (600 MHz, Methanol-d_4) δ 7.67 (d, *J* = 8.5 Hz, 2H), 7.35 (dt, *J* = 7.9, 0.9 Hz, 2H), 7.26 (d, *J* = 8.7 Hz, 2H), 7.08 (d, *J* = 8.5 Hz, 3H), 7.04 – 7.02 (m, 1H), 6.98 (ddd,

J = 8.1, 7.3, 1.1 Hz, 1H), 6.75 (d, *J* = 8.6 Hz, 2H), 5.41 (s, 2H), 3.96 (tt, *J* = 10.7, 4.0 Hz, 1H), 3.38 (m, 2H), 3.01 (m, 2H), 2.90 – 2.81 (m, 4H), 2.24 (m, 2H), 1.81 (m, 2H); ^{13}C NMR (151 MHz, MeOD) δ 155.9, 153.7, 142.2, 141.3, 133.8, 132.3 (2C), 129.3 (2C), 128.6, 127.1 (2C), 121.4, 119.8, 118.0, 115.1 (2C), 114.9, 111.0, 107.7, 59.2, 51.8 (2C), 48.8, 44.3, 30.7 and 30.2 (2C); LC-MS (APCI/ESI): found *m/z* = 452.1 $[M+H]^+$ (cal. for $C_{28}H_{29}N_5O$, 451.24); Purity: 98% (t_R = 0.587 min)

1-(4-fluorobenzyl)-N-(1-(3-methoxyphenethyl)piperidin-4-yl)-1H-benzo[d]imidazol-2-amine (18)

White solid (78%); ^{1}H-NMR (600 MHz, Methanol-d_4) δ 7.35 – 7.33 (d, *J* = 7.74 Hz, 1H), 7.20 (td, *J* = 1.7, 7.8 Hz, 1H), 7.18 – 7.13 (m, 3H), 7.08 – 7.00 (m, 4H), 6.96 (td, *J* = 8.1 and 1.1, Hz, 1H), 6.93 (dd, *J* = 8.2 and 1.0, Hz, 1H), 6.88 (td, *J* = 7.4 and 1.1 Hz, 1H), 5.26 (s, 2H), 3.88 (t, *J* = 10.9 Hz, 1H), 3.84 (s, 3H), 3.10 (d, *J* = 11.7 Hz, 2H), 2.94 – 2.77 (m, 2H), 2.76 – 2.63 (m, 2H), 2.40 (td, *J* = 12.2 Hz, 2H), 2.20 – 2.03 (m, 2H), and 1.77 – 1.58 (m, 2H); ^{13}C-NMR (151 MHz, MeOD) δ 162.20 (d, *J* = 244.58 Hz, C-F), 157.5, 153.9, 141.6, 134.0, 132.4 (d, *J* = 3.54 Hz), 129.9, 128.23 (d, *J* = 7.7 Hz, 2C), 127.5, 127.4, 121.1, 120.3, 119.5, 115.06 (d, *J* = 22 Hz, 2C), 114.7, 110.2, 107.7, 58.2, 54.4, 52.0 (2C), 49.7, 43.9, 31.1 (2C) and 27.2; LC-MS $(APCI/ESI)^+$, found *m/z* = 458.9 $[M+H]^+$ (calculated for $C_{28}H_{31}FN_4O$, 458.58); Purity = 99.16% (t_r = 2.487 min).

1-(4-fluorobenzyl)-N-(1-(2-methoxyphenethyl)piperidin-4-yl)-1H-benzo[d]imidazol-2-amine (19)

White solid (71%); ^{1}H-NMR (600 MHz, Methanol-d_4) δ 7.34 (d,J = 7.8 Hz, 1H), 7.20 (t, *J* = 8.0 Hz, 1H), 7.15 (m, 2H), 7.08 – 6.99 (m, 4H), 6.98-6-39 (m, 2H), 6.82 – 6.79 (m, 2H), 6.77 (dd, *J* = 2.4, 8.2 Hz, 1H), 5.25 (s, 2H), 3.86 (tt, *J* = 4.2, 10.8 Hz, 1H), 3.09-3.00 (m, 2H), 2.85-2.78 (m, 2H), 2.74 – 2.61 (m, 2H), 2.35 (t, *J* = 11.8 Hz, 2H), 2.18 – 2.07 (m, 2H), 1.67 (m, 2H); ^{13}C-NMR (151 MHz, MeOD) δ 162.20 (d, *J* = 244.58 Hz), 159.9, 153.9, 141.6, 141.2, 134.0, 132.4 (d, *J* =

2.66 Hz), 129.1, 128.23 (d, *J* = 8.1 Hz, 2C), 128.2, 121.1, 120.6, 119.5, 115.07 (d, *J* = 22 Hz, 2C), 114.7, 114.0, 111.3, 107.7, 59.8, 54.2, 52.1 (2C), 49.7, 43.9, 32.7 and 31.3 (2C); LC-MS $(APCI/ESI)^+$, found *m/z* = 458.9 $[M+H]^+$ (calculated for $C_{28}H_{31}FN_4O$, 458.58); Purity = 99.50% (t_r = 2.469 min).

1-(4-fluorobenzyl)-N-(1-phenethylpiperidin-4-yl)-1H-benzo[d]imidazol-2-amine (20)

White solid (79%); ^{1}H-NMR (600 MHz, Methanol-d_4) δ 7.34 (d, *J* = 7.8 Hz, 1H), 7.29 (t, *J* = 7.5 Hz, 1H), 7.25 – 7.17 (m, 3H), 7.17-7.12 (m, 2H), 7.08 – 6.99 (m, 4H), 6.96 (t, *J* = 7.6 Hz, 1H), 5.25 (s, 2H), 3.96 – 3.81 (m, 1H), 3.19 – 2.99 (m, 2H), 2.97 – 2.77 (m, 2H), 2.77 – 2.63 (m, 2H), 2.38 (t, *J* = 11.9 Hz, 2H), 2.13 (d, *J* = 13.0 Hz, 2H) and 1.69 (m, 2H); ^{13}C-NMR (151 MHz, MeOD) δ 163.0 and 161.4 (d, *J* = 244.58 Hz, C-F), 153.9, 141.5, 139.5, 134.0 (d, J = 2.3 Hz, 2C), 132.39 (d, *J* = 2.31 Hz), 128.3 (m, 3C), 128.2 (2C), 128.0, 125.9, 121.1, 119.5, 115.07 (d, *J* = 21.8 Hz), 114.7, 107.7, 59.9, 52.1 (2C), 49.7, 43.9, 32.6, 31.2 (2C); LC-MS $(APCI/ESI)^+$, found *m/z* = 428.9 $[M+H]^+$ (calculated for $C_{27}H_{29}FN_4$, 428.24); Purity = 99.57% (t_r = 2.452 min).

4-(2-(4-((1-(4-fluorobenzyl)-1H-benzo[d]imidazol-2-yl)amino)piperidin-1-yl)ethyl)phenol (DM-AST)

A solution of **AST** (0.1 grams, 0.02 mmol) in HBr (48%, 5 mL) was refluxed (120 °C) for 6 h. After completion of reaction, the reaction mixture was cooled to 0 °C and treated with 1 M aqueous NaOH in dropwise manner to neutralized excess of HBr (pH = 12-14). The organic components were extracted with 10% methanol in DCM (5 × 10 mL), and combined organic layers was dried over sodium sulfate. The removal of solvent under reduced pressure furnished DM-AST as an orange solid (0.4 grams, 45% yield); ^{1j}H-NMR (400 Hz, DMSO): δ_{ppm} 9.20 { bs, 1H, OH (disappears in D_2O shake)}, 7.24 (m, 3H), 7.15 (d, *J* = 8.0 Hz, 2H), 7.06 (d, *J* = 8.0 Hz, 1H), 7.02 (d, *J* = 8.4 Hz, 2H), 6.94 (t, *J* = 8.0 Hz, 1H), 6.84 (t, *J* = 7.6 Hz, 1H), 6.68 (d, *J* = 8.0 Hz, 2H), 6.50

(bs, 1H), 5.27 (s, 2H), 3.85 (m, 1H), 3.05 (m, 2H), 2.77-2.66 (m, 4H), 2.37 (m, 2H), 2.04 (m, 2H), 1.79-1.62 (m, 2H); ^{13}C-NMR (101 Hz, DMSO): 167.6, 161.90 (d, J = 243.0 Hz, C-F), 154.4, 143.3, 142.8, 134.8, 133.81 (d, J = 2.41 Hz), 129.9 (2C), 129.42 (d, J = 8.2 Hz, 2C), 121.0, 119.0, 115.74 (overlapping d, J = 18.9 Hz, 2C), 115.7 (3C), 108.3, 59.8, 52.3 (2C), 50.0, 44.4 (2C), 32.0 and 31.6; LC-MS (APCI/ESI)$^+$, found m/z = 445.2 $[M+H]^+$ (calculated for $C_{27}H_{29}FN_4O$, 444.23); Purity = 95.2%, (t_r = 2.635 min).

Material and method of *in vitro* Antiplasmodium **assay:**

(a) Parasite lactate dehydrogenase assay at UCT for *in Vitro* Antiplasmodium **Activity Testing:** All parasite strains were acquired from MR4 (Malaria Research and Reference reagent Resource Centre, Manassas, VA). Briefly, the respective stock solutions of CQ diphosphate and test compounds were prepared to 2 mg/mL in distilled water (for CQ) and 100% DMSO (for test compounds) then stored at -20 °C and further dilutions prepared on the day of the experiment. Synchronized trophozoite-stage cultures of *Pf*NF54 (CQS) and *Pf*K1 (CQR) were prepared to 2% parasitemia and 2% haematocrit. Compounds were tested at starting concentrations of 10 000 ng/mL (1 000 ng/mL for CQ), which were then serially diluted 2-fold in complete medium to give 10 concentrations with a final volume of 200 µL in each well. Parasites were incubated in the presence of the compounds at 37 °C and under normal hypoxic conditions for 48 h. Following incubation, 100 µL of MalStat reagent and 15 µL of re-suspended culture were combined, followed by addition of 25 µL of NBT (nitro blue tetrazolium chloride). The plates were kept in the dark for about 10 min to fully develop and absorbance measured at 620 nm on a microplate reader. Raw data were exported to Microsoft Excel for dose-response analysis.

(b) Modified [^{3}H]-hypoxanthine incorporation assay at Swiss TPH for *in vitro* antiplasmodium activity testing: Compounds were screened against multidrug resistant (*Pf*K1) and sensitive

(*Pf*NF54) strains of *P. falciparum* in vitro using the modified [^{3}H]-hypoxanthine incorporation assay.[17] Plasmodium falciparum was cultivated in a variation of the medium previously described,[18,19] consisting of RPMI 1640 supplemented with 0.5% ALBUMAX® II, 25 mM Hepes, 25 mM $NaHCO_3$ (pH 7.3), 0.36mM hypoxanthine, and 100 microgram/ml neomycin. Human erythrocytes served as host cells. Cultures were maintained at 37 °C in an atmosphere of 3% O_2, 4% CO_2, and 93% N_2 in humidified modular chambers. Compounds were dissolved by sonication in DMSO (10mg/ml) and diluted in hypoxanthine-free culture medium. Infected erythrocytes (100 microliter per well with 2.5% haematocrit and 0.3% parasitemia) were added to each drug titrated in 100 microliter duplicates over a 64-fold range. After 48 h incubation, 0.5 microCi of [^{3}H] hypoxanthine in 50 microliter media was added and plates were incubated for an additional 24 h. Parasites were harvested onto glass-fibre filters and radioactivity was counted using a Beta plate liquid scintillation counter (Wallac, Zurich). The results were recorded as counts per minute (cpm) per well at each drug concentration and expressed as a percentage of the untreated controls. Fifty percent inhibitory concentrations (IC_{50}) were estimated by linear interpolation.[20]

***In Vitro* Gametocyte Activity Testing:** Gametocytes were produced as per method reported by Reader and co-workers.[21] Late stage gametocytocidal dual point screens and IC_{50} determination were cross-validated on the luciferase reporter and ATP bioluminescence platforms.[21] All assays were performed in parallel using the same stock compounds, diluted fresh with complete culture medium from 10 mM stock solutions in DMSO (0.5% v/v), and included methylene blue as drug control. IC_{50}s were generated with GraphPad Prism 6, for n=3 independent biological replicates performed in technical triplicates, ± S.E.

***In Vitro P. berghei* Liver Stage Assay:** Inhibition of liver stage infection by test compounds was assessed by measuring the luminescence intensity in Huh-7 cells infected with a firefly luciferase-expressing *P. berghei* ANKA parasite line, as previously described.[13]

Assay procedure: Briefly, Huh-7 cells, a human hepatoma cell line, were cultured in 1640 RPMI medium supplemented with 10% v/v fetal bovine serum, 1% v/v nonessential amino acids, 1% v/v penicillin/streptomycin, 1% v/v glutamine, and 10 mM 4-(2-hydroxyethyl)-1-piperazineethanesulfonic acid (HEPES), pH 7, and maintained at 37 °C with 5% CO_2. For infection assays, Huh-7 cells (1.0×10^4 per well) were seeded in 96-well plates the day before drug treatment and infection. The medium was replaced by infection medium (*i.e.* culture medium supplemented with gentamicin (50 μg/mL) and amphotericin B (0.8 μg/mL)) containing the appropriate concentration of each compound approximately 1 h prior to infection with sporozoites freshly obtained through disruption of salivary glands of infected female *Anopheles stephensi* mosquitoes. An amount of the DMSO solvent equivalent to that present in the highest compound concentration was diluted in infection medium and used as control. Sporozoite addition was followed by centrifugation at 1,700 grams for 5 min and subsequent incubation for 48 h at 37°C with 5% CO_2. The effect of the compounds on the viability of Huh-7 cells was assessed by the Alamar Blue assay (Invitrogen, U.K.) according to the manufacturers protocol, followed by measurement of parasite infection load by a bioluminescence assay (Biotium). Nonlinear regression analysis was employed to fit the normalized results of the dose-response curves, and IC_{50} values were determined using GraphPad Prism 6.0.

Cytotoxicity Testing: Compounds were screened for *in vitro* cytotoxicity against Chinese Hamster Ovarian (CHO) mammalian cell-lines, using the 3-(4,5-dimethylthiazol-2-yl)-2,5-diphenyltetrazoliumbromide (MTT)-assay. The reference standard, emetine, was prepared to 2

mg/mL in distilled water while stock solutions of test compounds were prepared to 20 mg/mL in 100% DMSO with the highest concentration of solvent to which the cells were exposed having no measurable effect on the cell viability. The initial concentration of the compounds and control was 100 μg/mL, which was serially diluted in complete medium with 10-fold dilutions to give 6 concentrations, the lowest being 0.001 μg/mL. Plates were incubated for 48 h with 100 μL of drug and 100 μL of cell suspension in each well and developed afterwards by adding 25 μL of sterile MTT (Thermo Fisher Scientific) to each well and followed by 4 h incubation in the dark. The plates were then centrifuged, medium aspirated and 100 μL DMSO added to dissolve crystals before reading absorbance at 540 nm. Data were analysed, and sigmoidal dose-response derived using GraphPad Prism v 4.0 software (La Jolla, USA). All experiments were performed for at least three independent biological repeats, each with technical triplicates.

Inhibition of β-haematin Formation: Briefly, stock solutions of control (CQ and AQ) and test compounds were made to 20 mM in 100% DMSO. A solution containing water/305.5 μM NP40/DMSO at a v/v ratio of 70%/20%/10%, respectively was added to every well in columns 1-11 of a 96-well plate while 140 μL of water and 40 μL of 305.5 μM. NP40 were added to column 12 to mediate the formation of β-haematin. 20 μL of control or test compound (20 mM) was added to column 12 and 100 μL of this solution serially diluted to column 2, with column 1 left as a blank (0 μM compound). A 178.8 μL aliquot of haematin stock was suspended in 20 mL of a 1 M acetate buffer, pH 4.9 and 100 μL of this haematin suspension added into each well. Plates were then incubated for ~5 h at 37 °C after which 32 μL of pyridine solution (20% water, 20% acetone, 10% 2 M HEPES buffer pH 7.4, 50% pyridine) was added followed by addition of 60 μL of acetone to all wells. Plates were read at 405 nm and dose-response curves plotted in GraphPad Prism v.6 (GraphPad Software Inc., La Jolla, USA) to obtain IC_{50}s values.

Cellular heme fractionation assay: Cultures were synchronized at 48 h intervals with 5% (w/v) sorbitol, and ring-stage parasites incubated with the test drugs at various multiples of their IC_{50}s. RBCs were then harvested after 32 h, and the trophozoites were isolated with 0.05% (wt/vol) saponin and washed with 1× PBS (pH 7.5) to remove traces of the RBC haemoglobin. RBCs and trophozoites were quantified in these samples using a haemocytometer and flow cytometry. The contents of the trophozoite pellet were then released by hypotonic lysis and sonication. Following centrifugation, the supernatants corresponding to membrane-soluble haemoglobin fraction were treated with 4% (w/v) SDS, and 2.5% (v/v) pyridine. The pellets were again treated with 4% SDS, 25% pyridine, sonicated and centrifuged. Supernatants corresponding to the 'free' heme fraction were then carefully recovered. The remaining pellets (hemozoin fraction) were then solubilized in 4% SDS, 0.3 M NaOH and then neutralized with 0.3 M HCl, sonicated, and treated with 25% pyridine. The UV-visible spectrum of each heme fraction as an Fe(III) heme -pyridine complex was measured using a multiwell plate reader (Spectramax 340PC; Molecular Devices). The total amount of each heme species was quantified using a heme standard curve,[16] whereby the mass of each heme Fe species per trophozoite was calculated by dividing the total amount of each heme species by the corresponding number of parasites in that fraction as determined by flow cytometry.[16] Statistical comparisons were made using Students t-test on GraphPad Prism 6 software (GraphPad Software Inc., La Jolla, USA).[16]

Kinetic Solubility: The kinetic solubility assay was performed using a miniaturized shake flask method as previously described (Hill AP and Young RJ, 2010). Briefly, 10 mM stock solutions of each of the compounds were used to prepare calibration standards (10-220 μM) in DMSO. The same 10 mM stock solutions were accurately dispensed in duplicate into 96-well plates and the DMSO dried down (MiVac GeneVac, 90 min, 37 ˚C). Thereafter, the samples were reconstituted

(200 μM) in aqueous solution and shaken (20 hours, 25 °C). The solutions were analysed by means of HPLC-DAD (Agilent 1200 Rapid Resolution HPLC with a diode array detector). Best fit calibration curves were constructed using the calibration standards, which were used to determine the aqueous solubility of the samples.

LC-MS: The LC purity traces were performed using one of the following methods:

Method 1: Using a Kinetex 2.6 μM C-18 column, 2 μL injection volume, flow 0.7 mL/min; gradient: 15-100% B in 1.2 min (hold 3.3 min), 100-15% in 0.3 min (hold 1.2 min) (Mobile phase A: 10 mM buffer (Ammonium acetate/acetic acid) in H_2O and Mobile phase B: 10 mM buffer (Ammonium acetate/acetic acid) in Methanol).

Method 2: Using a Kinetex 1.7 μM C-18 column, 1 μL injection volume, flow 1.2 mL/min; gradient: 5-100% B in 1.5 min (hold 0.4 min), 100-5% in 0.3 min (hold 0.5 min) (Mobile phase A: 0.1% formic acid in H_2O and Mobile Phase B: 0.1% formic acid in Acetonitrile).

Supplementary Information: Additional details of the structures of all derivatives assessed are provided as Supplementary material. Excel file with the compounds SMILES format is also provided.

Acknowledgements: The University of Cape Town (KC), South African Medical Research Council (KC, TJE, LMB and TLC), and South African Research Chairs Initiative of the Department of Science and Technology (KC: UID 64767 and LMB: UID84627), administered through the South African National Research Foundation, are gratefully acknowledged for support.

At Swiss TPH, we thank Christoph Fischli, Sibylle Sax and Christian for assistance in performing the [^{3}H]-hypoxanthine incorporation assay.

REFERENCES:

(1) W. H. O. *World Malaria Report 2017*; 2017.

(2) Ashley, E. A.; Dhorda, M.; Fairhurst, R. M.; Amaratunga, C.; Lim, P.; Suon, S.; Sreng, S.; Anderson, J. M.; Mao, S.; Sam, B.; Sopha, C.; Chuor, C. M.; Nguon, C.; Sovannaroth, S.; Pukrittayakamee, S.; Jittamala, P.; Chotivanich, K.; Chutasmit, K.; Suchatsoonthorn, C.; Runcharoen, R.; Hien, T. T.; Thuy-Nhien, N. T.; Thanh, N. V.; Phu, N. H.; Htut, Y.; Han, K.-T.; Aye, K. H.; Mokuolu, O. A.; Olaosebikan, R. R.; Folaranmi, O. O.; Mayxay, M.; Khanthavong, M.; Hongvanthong, B.; Newton, P. N.; Onyamboko, M. A.; Fanello, C. I.; Tshefu, A. K.; Mishra, N.; N. Valecha; Phyo, A. P.; Nosten, F.; Yi, P.; Tripura, R.; Borrmann, S.; Bashraheil, M.; Peshu, J.; Faiz, M. A.; Ghose, A.; Hossain, M. A.; Samad, R.; Rahman, M. R.; Hasan, M. M.; Islam, A.; Miotto, O.; Amato, R.; MacInnis, B.; Stalker, J.; Kwiatkowski, D. P.; Bozdech, Z.; Jeeyapant, A.; Cheah, P. Y.; Sakulthaew, T.; Chalk, J.; Intharabut, B.; Silamut, K.; Lee, S. J.; Vihokhern, B.; Kunasol, C.; Imwong, M.; Tarning, J.; Taylor, W. J.; Yeung, S.; Woodrow, C. J.; Flegg, J. A.; Das, D.; Smith, J.; Venkatesan, M.; Plowe, C. V.; Stepniewska, K.; Guerin, P. J.; Dondorp, A. M.; Day, N. P.; White, N. J. Spread of Artemisinin Resistance in Plasmodium Falciparum Malaria. *N. Engl. J. Med.* **2015**, *371* (5), 411–423. DOI:10.1056/NEJMoa1314981.

(3) Edi, C. V. A.; Koudou, B. G.; Jones, C. M.; Weetman, D.; Ranson, H. Multiple-Insecticide Resistance in Anopheles Gambiae Mosquitoes, Southern Côte d'Ivoire. *Emerg. Infect. Dis.* **2012**, *18* (9), 1508–1511. DOI:10.3201/eid1809.120262.

(4) Njoroge, M.; Njuguna, N. M.; Mutai, P.; Ongarora, D. S. B.; Smith, P. W.; Chibale, K. Recent Approaches to Chemical Discovery and Development against Malaria and the

Neglected Tropical Diseases Human African Trypanosomiasis and Schistosomiasis. *Chem. Rev.* **2014**, *114* (22), 11138–11163. DOI: 10.1021/cr500098f.

(5) Chong, C. R.; Chen, X.; Shi, L.; Liu, J. O.; Sullivan, D. J. A Clinical Drug Library Screen Identifies Astemizole as an Antimalarial Agent. *Nat. Chem. Biol.* **2006**, *2* (8), 415–416. DOI: 10.1038/nchembio806.

(6) Meuldermans, W.; Hendrickx, J.; Lauwers, W.; Hurkmans, R.; Swysen, E.; Heykants, J. Excretion and Biotransformation of Astemizole in Rats, Guinea-Pigs, Dogs, and Man. *Drug Dev. Res.* **1986**, *8* (1–4), 37–51. DOI: 10.1002/ddr.430080106.

(7) Musonda, C. C.; Whitlock, G. A.; Witty, M. J.; Brun, R.; Kaiser, M. Chloroquine-Astemizole Hybrids with Potent in Vitro and in Vivo Antiplasmodial Activity. *Bioorg. Med. Chem. Lett.* **2009**, *19* (2), 481–484. DOI: 10.1016/j.bmcl.2008.11.047.

(8) Roman, G.; Crandall, I. E.; Szarek, W. A. Synthesis and Anti-Plasmodium Activity of Benzimidazole Analogues Structurally Related to Astemizole. *ChemMedChem* **2013**, *8* (11), 1795–1804. DOI: 10.1002/cmdc.201300172.

(9) Tian, J.; Vandermosten, L.; Peigneur, S.; Moreels, L.; Rozenski, J.; Tytgat, J.; Herdewijn, P.; Van den Steen, P. E.; De Jonghe, S. Astemizole Analogues with Reduced HERG Inhibition as Potent Antimalarial Compounds. *Bioorg. Med. Chem.* **2017**, *25* (24), 6332–6344. DOI: 10.1016/j.bmc.2017.10.004.

(10) Derbyshire, E. R.; Prudencio, M.; Mota, M. M.; Clardy, J. Liver-Stage Malaria Parasites Vulnerable to Diverse Chemical Scaffolds. *Proc. Natl. Acad. Sci.* **2012**, *109* (22), 8511–8516. DOI: 10.1073/pnas.1118370109.

(11) Van der Zee, J.; Barr, D. P.; Mason, R. P. ESR Spin Trapping Investigation of Radical Formation from the Reaction between Hematin and Tert-Butyl Hydroperoxide. *Free Radic. Biol. Med.* **1996**, *20* (2), 199–206. DOI: 10.1016/0891-5849(95)02031-4

(12) Schmitt, T. H.; Frezzatti, W. A.; Schreier, S. Hemin-Induced Lipid Membrane Disorder and Increased Permeability: A Molecular Model for the Mechanism of Cell Lysis. *Arch. Biochem. Biophys.* **1993**, *307* (1), 96–103. DOI: 10.1006/abbi.1993.1566.

(13) Ploemen, I. H. J.; Prudêncio, M.; Douradinha, B. G.; Ramesar, J.; Fonager, J.; Van Gemert, G. J.; Luty, A. J. F.; Hermsen, C. C.; Sauerwein, R. W.; Baptista, F. G.; Mota, M. M.; Waters, A. P.; Que, I.; Lowik, C. W. G. M.; Khan, S. M.; Janse, C. J.; Franke-Fayard, B. M. D. Visualisation and Quantitative Analysis of the Rodent Malaria Liver Stage by Real Time Imaging. *PLoS One* **2009**, *4* (11), 1–12. DOI: 10.1371/journal.pone.0007881.

(14) Mann, K. V; Crowe, J. P.; Tietze, K. J. Nonsedating Histamine H1-Receptor Antagonists. *Clin. Pharm.* **1989**, *8* (5), 331–344.

(15) Ncokazi, K. K.; Egan, T. J. A Colorimetric High-Throughput Beta-Hematin Inhibition Screening Assay for Use in the Search for Antimalarial Compounds. *Anal. Biochem.* **2005**, *338* (2), 306–319. DOI: 10.1016/j.ab.2004.11.022.

(16) Combrinck, J. M.; Fong, K. Y.; Gibhard, L.; Smith, P. J.; Wright, D. W.; Egan, T. J. Optimization of a Multi-Well Colorimetric Assay to Determine Haem Species in Plasmodium Falciparum in the Presence of Anti-Malarials. *Malar. J.* **2015**, *14*, 253. DOI: 10.1186/s12936-015-0729-9.

(17) Snyder, C.; Chollet, J.; Santo-Tomas, J.; Scheurer, C.; Wittlin, S. In Vitro and in Vivo

Interaction of Synthetic Peroxide RBx11160 (OZ277) with Piperaquine in Plasmodium Models. *Exp. Parasitol.* **2007**, *115* (3), 296–300. DOI: 10.1016/j.exppara.2006.09.016.

(18) Dorn, A.; Stoffel, R.; Matile, H.; Bubendorf, A.; Ridley, R. G. Malarial Haemozoin/Beta-Haematin Supports Haem Polymerization in the Absence of Protein. *Nature* **1995**, *374* (6519), 269–271. DOI: 10.1038/374269a0.

(19) Trager, W.; Jensen, J. B. Human Malaria Parasites in Continuous Culture. *Science* **1976**, *193* (4254), 673–675. DOI: 10.1126/science.781840.

(20) Huber, W.; Koella, J. C. A Comparison of Three Methods of Estimating EC50 in Studies of Drug Resistance of Malaria Parasites. *Acta Trop.* **1993**, *55* (4), 257–261. DOI: 0.1016/0001-706X(93)90083-N.

(21) Reader, J.; Botha, M.; Theron, A.; Lauterbach, S. B.; Rossouw, C.; Engelbrecht, D.; Wepener, M.; Smit, A.; Leroy, D.; Mancama, D.; Coetzer, T. L.; Birkholtz, L. Nowhere to Hide: Interrogating Different Metabolic Parameters of Plasmodium Falciparum Gametocytes in a Transmission Blocking Drug Discovery Pipeline towards Malaria Elimination. *Malar. J.* **2015**, *14* (1), 213. DOI: 10.1186/s12936-015-0718-z.

For Table of Contents Use Only